NASA CONTRACTOR REPORT

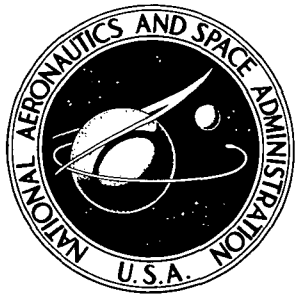

NASA CR-2529

NASA CR-2529

STUDY OF THE REACTION OF ATOMIC OXYGEN WITH AEROSOLS

Francis I. Akers and James P. Wightman

Prepared by
VIRGINIA POLYTECHNIC INSTITUTE AND STATE UNIVERSITY
Blacksburg, Va. 24061
for Langley Research Center

NATIONAL AERONAUTICS AND SPACE ADMINISTRATION • WASHINGTON, D. C. • MAY 1975

1. Report No.	2. Government Accession No.	3. Recipient's Catalog No.
NASA CR-2529		

4. Title and Subtitle	5. Report Date
"STUDY OF THE REACTION OF ATOMIC OXYGEN WITH AEROSOLS"	May 1975
	6. Performing Organization Code

7. Author(s)	8. Performing Organization Report No.
Francis I. Akers and James P. Wightman	

9. Performing Organization Name and Address	10. Work Unit No.
Virginia Polytechnic Institute and State University Blacksburg, VA	160-44-64-05-00
	11. Contract or Grant No. NAS 1-10646-20

12. Sponsoring Agency Name and Address	13. Type of Report and Period Covered
National Aeronautics and Space Administration Washington, D.C. 20546	Contractor Report
	14. Sponsoring Agency Code

15. Supplementary Notes

Final report

16. Abstract

The rate of disappearance of atomic oxygen has been measured at several pressures in a fast flow pyrex reactor system with its walls treated with $(NH_4)_2SO_4$ (s), H_2SO_4 (ℓ), and NH_4Cl (s). Atomic oxygen (^3P) was generated by dissociation of pure, low pressure oxygen in a microwave discharge (2.45 GHz). Concentrations of atomic oxygen were measured at several stations in the reactor system using chemiluminescent titration with NO_2. Recombination efficiencies calculated from experimentally determined wall recombination rate constants are in good agreement with reported values for clean Pyrex and an H_2SO_4 coated wall. The recombination efficiency for $(NH_4)_2SO_4$, the first reported value for this coating, results in a slightly lower value than for H_2SO_4. A rapid exothermic reaction between atomic oxygen and the NH_4Cl wall coating prevented recombination efficiency determination for this coating. Furthur experimentation with NH_4Cl aerosol flowing in the system with atomic oxygen resulted in a reaction rate between these two species which compares closely with an upper limit rate constant calculated from the model of Judeikis and Siegel. The data obtained in this study show that the technique is highly useful for wall recombination measurements and appears capable for use as a means of extrapolating to the case of free stream aerosol-gas interactions.

17. Key Words (Suggested by Author(s))	18. Distribution Statement
Aerosols Atomic Oxygen Recombination Chemical kinetics Aerosol-gas kinetics	Unclassified - Unlimited New Subject Category 72

19. Security Classif. (of this report)	20. Security Classif. (of this page)	21. No. of Pages	22. Price*
Unclassified	Unclassified	111	$5.25

*For sale by the National Technical Information Service, Springfield, Virginia 22151

TABLE OF CONTENTS

Chapter Page

LIST OF TABLES

LIST OF FIGURES

CHAPTER I

INTRODUCTION

The earth's atmosphere may be divided into several thermal layers known as the troposphere, stratosphere, mesosphere, and thermosphere. The stratosphere is that region lying roughly between 10 and 50 km altitude. The pressure in this layer decreases from 230 torr to about 0.75 torr, while the temperature increases from about 215 ^{o}K at the tropopause to around 270 ^{o}K at the stratopause. The stratosphere is quite important to life because of its ability to shield the earth's surface from biologically damaging radiation. This is due in part to the absorption of ultraviolet radiation by ozone (1-3). It is of interest therefore to study chemical reactions which may occur in the stratosphere and lead to significant reductions of ozone. Increasing amounts of aerosols such as H_2SO_4 and $(NH_4)_2SO_4$ have been detected in the stratosphere (4-6).

The present work is concerned with the effects of some aerosols on the recombination kinetics of atomic oxygen, a reactant necessary for the formation of ozone (7-8). The main objective was to measure atomic oxygen disappearance in a flow system having clean and coated walls; and in the

presence of NH_4Cl and $(NH_4)_2SO_4$ aerosols. Related studies performed included: characterization of coated reactor wall samples by electron spectroscopy for chemical analysis (ESCA), mass spectrometric analysis of the products of the reaction between $NH_4Cl(s)$ and atomic oxygen, and characterization of the aerosols using scanning electron microscopy.

CHAPTER II

REVIEW OF THE LITERATURE

Atomic Oxygen Formation and Recombination

The reactions of oxygen in the stratosphere will be reviewed briefly. Chapman (8) first suggested the "ozone mechanism" in 1930:

$$O_2 + h\upsilon \longrightarrow 2\ O \qquad [1]$$

$$O + O_2 + M \longrightarrow O_3 + M \qquad [2]$$

$$O_3 + h\upsilon \longrightarrow O + O_2 \qquad [3]$$

$$O_3 + h\upsilon \longrightarrow O(^1D) + O_2 \qquad [4]$$

$$O + O_3 \longrightarrow 2\ O_2 \qquad [5]$$

These reactions have been cited often as the only ones of importance concerning oxygen in the stratosphere (9,10), with the possible inclusion of

$$O + O + M \longrightarrow O_2 + M \qquad [6]$$

which becomes important if the atomic oxygen concentration is greater than about 10%. In the late sixties however, controversy over the environmental effects of a supersonic transport (SST) prompted research showing the importance of such species as CO, NO_x, and H_2O as reactants or "sinks" for atomic oxygen (11-13). Currently, authors list many reactions of oxygen species important to stratospheric chemistry (7, 14-18), including Crutzen, who gives 69 such

reactions. The ozone mechanism of Chapman is still used, however, for stratospheric modeling (3).

Several types of systems have been used for laboratory studies of atomic oxygen kinetics, depending on the particular phenomenon to be observed. Several reviews exist (18-21), and list primarily (a) discharge-flow systems, (b) static systems with pulsed radiolysis, (c) flash photolysis-resonance fluorescence apparatus, (d) shock tubes, and (e) thermal decomposition-stirred flow reactors. Some of the studies of the homogeneous recombination of oxygen have used methods such as (b) and (c) (22, 23) but the preponderance of studies have been done using discharge-flow systems, especially with microwave discharges (2450 MHz).

Discussions of reactions in discharge-flow systems, such as those by Wightman (24) and Thrush (25) summarize the area, while the specifics of atom production in a microwave discharge are well covered by Kaufman (26) and Bell and Kwong (27). The atomic oxygen produced by a microwave discharge through pure oxygen is essentially all in the ground state, ^3P (28). This was verified by Herron and Huie (29) who found no O('D) or O('S). The discharge also produces excited molecular oxygen. Those species found are $O_2(^1\Delta g)$ and $O_2(^1\Sigma g^+)$ (29, 30). The concentration of $O_2(^1\Delta g)$ typically is about 5%, while

the amount of $O_2(^1\Sigma g^+)$ is much less than 5% (30).

Measurement of atomic oxygen concentration for kinetic studies in discharge-flow systems was reviewed by some of the authors above (18-24). Kaufman (31, 32) fully developed the "NO_2 titration" technique suggested by Spealman and Rodebush (33). In this often used method, NO_2 is allowed to mix with a gas stream containing atomic oxygen, and the following reactions take place:

$$O + NO_2 \longrightarrow NO + O_2 \qquad [7]$$

$$O + NO \longrightarrow NO_2 + h\upsilon \qquad [8]$$

Reaction [7] is very fast, so that when the flow of NO_2 is one-half that of the atomic oxygen, a maximum in the chemiluminescent glow is obtained. When the flow of NO_2 is just equal to the flow of atomic oxygen, the glow is sharply extinguished throughout the flow tube. This reaction is quite specific for oxygen atoms, and by measuring the flow of NO_2, an absolute estimate of the atomic oxygen concentration can be made (18). Limitations of this method above a system pressure of two torr are discussed by Mearns and Morris (34), and at low concentrations by Slagle et al. (35). Other atomic oxygen measurement methods include catalytic probes (18), Wrede-Harteck gauges (18), ESR (36-38), resonance fluorescence (22), time resolved IR (23), and mass spectrometry (29).

The mechanisms and kinetics of atomic oxygen recombination have been studied extensively since they are of great aeronomic interest. The predominant homogeneous mechanism seems to be the previously mentioned "ozone mechanism" (18, 21):

$$O + O_2 + M \xrightarrow{k_{GAS}} O_3 + M \qquad [2]$$

followed by

$$O_3 + O \xrightarrow{k_5} 2\ O_2 \qquad [5]$$

When numerical rate constant subscripts appear, they refer to the equation number used in the text. In flow tubes, heterogeneous wall recombination is also significant. Several studies show this to be a unimolecular first order process expressed as:

$$O + \text{Wall} \xrightarrow{k_{WALL}} 1/2\ O_2 + \text{Wall} \qquad [9]$$

Several mechanisms have been proposed to explain this first order atom disappearance (18, 28, 39). The actual observed decay of atomic oxygen with time in a flow tube is pseudo-first-order. That is, plots of ln [O] versus time (distance divided by flow velocity) are linear. This has been interpreted in terms of the ozone model plus wall recombination in various ways. Kaufman (18) and Francis (37) assume an ozone steady state, such that:

$$-d[O]/dt = k_{GAS}\,[O][O_2]^2 + k_5[O_3][O] + k_{WALL}\,[O] \qquad [10]$$

$$d[O_3]/dt = k_{GAS}[O][O_2]^2 - k_5[O_3][O] \qquad [11]$$

and

$$d[O_3]/dt = 0. \qquad [12]$$

Now,

$$k_5[O_3][O] = k_{GAS}[O][O_2]^2 \qquad [13]$$

and

$$-d[O]/dt = 2k_{GAS}[O][O_2]^2 + k_{WALL}[O] \qquad [14]$$

The rate constant for the pseudo-first-order atom disappearance, k_{APP}, is thus given by

$$k_{APP} = k_{WALL} + 2k_{GAS}[O_2]^2 \qquad [15]$$

Several authors (18, 37, 38) have used this relation by measuring k_{APP} as a function of molecular oxygen concentration. The intercept of a plot of k_{APP} versus the square of the oxygen pressure is taken as k_{WALL} and the slope as twice the rate constant, k_{GAS}, for the homogeneous gas phase recombination. Other authors disagree with the idea of an ozone steady state, and cite the following three reactions:

1. the catalytic removal of atomic oxygen by hydrogenous impurities (40-43):

$$H + O_2 + M \longrightarrow HO_2 + M \qquad [16]$$

$$O + HO_2 \longrightarrow OH + O_2 \qquad [17]$$

$$O + OH \longrightarrow H + O_2 \qquad [18]$$

2. The regeneration of atomic oxygen by reaction of

ozone with metastable states of molecular oxygen for the discharge (40-44):

$$O_3 + O_2(^1\Sigma g^+ \text{ or } ^1\Delta g) \longrightarrow O(^3P) + 2\ O_2 \qquad [19]$$

3. the loss of atomic oxygen by reaction with polyatomic ions formed in the discharge (26):

$$O_4^+ + O \longrightarrow O_3^+ + O_2 \qquad [20]$$

$$O_3^+ + O \longrightarrow O_2^+ + O_2 \qquad [21]$$

The experimental evidence shows nonetheless that plots of k_{APP} versus molecular oxygen concentration are linear. This linearity has been explained by Schiff (45), Mearns and Morris (46) and Clyne (47) who propose that if hydrogen is present in the oxygen, the following reaction takes place:

$$H + O_3 \longrightarrow OH + O_2 \qquad [22]$$

$$O + OH \longrightarrow O_2 + H \qquad [23]$$

Reaction [22] is very fast and quickly uses up any ozone formed. The net kinetic effect is the same as equation [14].

The wall recombination rate has been determined in two ways: (a) by plotting k_{APP} values obtained at different pressures versus oxygen pressure squared, and extrapolating to zero pressure (18, 37, 38, 46), or (b) by measuring k_{APP} at low pressures (<1 torr) and assuming atom decay to be predominantly due to wall recombination (29, 37, 47):

$$k_{APP} \approx -d \ln[O]/dt \qquad [24]$$

Values of k_{WALL} are usually reported in terms of γ, the fraction of wall collisions leading to recombination. γ is calculated for a cylindrical reactor tube from

$$k_{WALL} = \gamma \bar{v}/d \qquad [25]$$

and rearranging to

$$\gamma = k_{WALL} d/\bar{v} \qquad [26]$$

where d is the tube diameter and $\bar{v}$ is the root mean square molecular velocity of the atoms (18, 29, 48). Values of γ have been determined and can be used for selection of an effective wall coating to prolong atomic oxygen and ozone lifetimes in various apparatus (18, 48).

Finally, a brief discussion on the use of fast flow techniques to study reaction kinetics is in order. Excellent reviews on this topic have been written by Kaufman (18), Clyne (47), and Francis (37). These authors specify how a flow system may be constructed and operated so as to minimize its limitations. Important assumptions that must be made concerning flow problems, along with means of evaluation of their contributions are given below. The assumptions are:

(1) assumption of negligible pressure drop down the reactor tube, as found from the simplified expression for Poiseuille flow:

$$\Delta P/l = 1.18 \times 10^{-6}(u/r^2) \qquad [27]$$

ΔP is in torr, l is tube length in cm, u is the linear gas velocity in cm/sec, and r is the tube radius in centimeters.

(2) assumption of negligible back diffusion and axial concentration gradients, the necessary relation being

$$Dk/u^2 << 1 \qquad [28]$$

where D is the diffusion coefficient of oxygen atoms into the gas, and k is the observed rate of atom disappearance;

(3) assumption of small radial concentration gradients. Kaufman (19) calculates that for a 2 cm diameter flow tube operating at 1 torr and room temperature, atom concentration differences from tube center to wall are < 1%. This can be larger and become important at higher pressures and in larger diameter tubes.

Aerosol Formation and Characterization

In 1961, Junge et al. (4) presented the first evidence for the existence of aerosols in the stratosphere. Since that time, numerous studies have verified the presence of aerosols in the stratosphere, and have identified the major components of these aerosols as H_2SO_4 and $(NH_4)_2SO_4$ (5, 49). These studies showed the maximum aerosol concentration to lie in a band from 15 to 23 km with a maximum at 20 km. The average particle density was about 0.1 cm^{-3}, with a particle size range between 0.1 and 2 μm. Currently,

aerosol concentrations are measured in $\mu g/m^3$ (50). Other researchers have attempted to show how these aerosols form (51, 52). Kiang (53) offered a mechanism for the formation of $(NH_4)_2SO_4$ aerosol and speculated on the possibility of forming NH_4Cl aerosol with increasing concentrations of HCl. Wofsy and McElroy (54) indicated that aerosol formation could be an important sink for NH_3 in the stratosphere by reacting with HCl to form NH_4Cl, and called for studies of that system. Stolarski and Cicerone (55) have indicated that HCl is the predominant chlorine species in the stratosphere. Some good reviews which discuss general characteristics of stratospheric as well as other aerosols are given by First (56), Lee (57), Mossop (5), and Mueller and Kothny (55).

In the laboratory, several methods exist for the formation of aerosols for study, including vapor condensation, atomization, and gas phase chemical reaction (58). Goetz and Pueschel (59) used a nebulizer, Berglund and Liu (60) developed a vibrating orifice monodisperse aerosol generator, and Dahneke (61) described an aerosol beam spectrometer. Aerosol generation for studies of nucleation and growth were carried out by Twomey (62), who formed NH_4Cl particles over aqueous solutions of HCl and NH_3, and Scargill (63) who reacted NH_3 and SO_2 in the gas phase.

Scargill (63) found that solid products formed only in the presence of water vapor. Kiang, Stauffer, and Mohen (53), working with "atmospheric concentrations" of NH_3 and HCl found NH_4Cl particles formed in the presence of other ions. Countess and Heicklen (64) did an exhaustive study on the gas phase reaction of NH_3 with HCl. They used a flow apparatus, operating at 25 °C and 1 atm. They showed that although monomeric NH_4Cl forms and can act as a nucleating agent, it primarily condenses on particles already formed. The rate constant, k, in the expression

$$-dn/dt = k[NH_3][HCl] \qquad [29]$$

where n is the number of molecules of either reactant, was determined to be 1.9×10^{-17} cm^3/molecule sec. By varying reactant concentrations, they showed by product analysis that no entrapment of excess gases occurred. Friend et al. (51) studied the formation of $(NH_4)_2SO_4$ aerosols by reaction of NH_3, SO_2, H_2O and O_3 in various proportions and with different amounts of UV radiation. They found that radiation was necessary for sizable particle formation. Robbins and Cadle (65) formed an $(NH_4)_2SO_4$ aerosol by reacting NH_3 with H_2SO_4 aerosol. They found a relation between complete reaction time and drop size, and determined that the rate of reaction was controlled by diffusion inside the H_2SO_4 droplets.

Analysis of aerosols is usually performed by standard

methods after collection (66). The chemical analysis of aerosols was reviewed by Mueller and Kothny (50). Collection of aerosol particles has been studied extensively. Ranz and Wong (67) list the mechanisms of collection as (a) inertia, (b) interception, (c) electrical attraction, and (d) settling. They discuss models for inertial impaction, as do Golovin and Putnum (68), Dahneke (69), Dahneke and Flachsbart (70), and Friedlander (71).

Interactions Between Aerosols and Gases

No experimental studies of reactions between aerosols and atoms could be found in the literature. Olivero (72) has concluded from a theoretical study that particle catalysed recombination may compete with gas phase recombination of atomic oxygen in the mesosphere. The author based his calculation on a collision model, making assumptions as to the efficiency for adsorption and recombination of oxygen atoms and the chemical and physical characteristics of the aerosol. Olivero indicated a need for information on efficiency of recombination upon collision and on aerosol characteristics.

Very few studies have been carried out for aerosol-gas systems, even though some authors have commented on the scarcity of data (73, 74). There may be synergistic effects or enhanced rates of reactions in the presence

of aerosols which are of concern in atmospheric pollution (75-77). Barr et al. (78) studied reactions of NaCl crystals with H_2O, O_2, and O_3 and pointed out that the extent of the reactions was much greater than would be predicted by thermodynamic properties of the bulk phases. Johnstone and Coughanour (79) made drops of catalytic solutions and measured rates of SO_2 oxidation in the suspended drops. The drops contained H_2O_2 or $MnSO_4$ and the catalytic rate of oxidation of SO_2 was about 500 times faster than the photochemical oxidation of SO_2. Actual aerosol-gas reactions were studied by Robbins, Cadle, and Eckhardt (80), and Robbins and Cadle (65). Products were determined for the following aerosol-gas systems: (a) $NaCl$-NO_2, (b) $NaNO_3$-$NOCl$, (c) $NaCl$-HNO_3, (d) $NaNO_3$-HCl, and (e) $CaCl_2$-NO_2. In addition to product analysis, the kinetics of the aerosol-gas reaction of H_2SO_4-NH_3 were studied by Robbins and Cadle (65). Cadle (81) summarized the above reactions and discussed their general kinetics. He proposed a model for the upper limit of the reaction rate taken from collision theory. The number of collisions of gas species per second per unit area of particle surface was estimated assuming a steric factor P = 1 and an activation energy E = 0. The rate expression for surface controlled reactions is given by

$$-d[A]/dt = 3k[A]_o[B]_o/r_o \qquad [30]$$

where [A] is the reactive gas concentration, [B] is the aerosol concentration in weight or volume units, and r is the radius of a spherical particle. The rate constant, k, is given by

$$k = PZ\exp(-E/RT) \qquad [31]$$

where Z is the collision number.

Judeikis and Siegel (77) reviewed aerosol-gas interactions and used a model for calculating the efficiency of particle-catalysed removal of gases, either through adsorption or reaction. They gave the expression for the frequency of collisions between gas molecules G and aerosols with a surface area per unit volume A as:

$$k_c[G]A = (RT/2\pi M_G)^{\frac{1}{2}}[G]A \qquad [32]$$

where M_G is the gas molecular weight. They assumed only a fraction, Φ, of the collisions lead to removal of G, and wrote

$$-d[G]/dt = \Phi k_c[G]A = \Phi(RT/2\pi M_G)^{\frac{1}{2}}[G]A \qquad [33]$$

For A, they substituted the expression:

$$A = 3\gamma W/\rho r_m \qquad [34]$$

where γ is a factor related to the form of the particle size distribution (usually $\gamma = 2\pm1$), W is the mass of particles per unit volume with density ρ, and r_m is the mean radius of the particles. Combining equations [34] - [35] yields

$$-d[G]/dt = 3\Phi\gamma W/\rho r_m(RT/2\pi M_G)^{\frac{1}{2}}[G]. \qquad [35]$$

The authors go on to substitute mean values for the variables and solve for Φ in order to predict how efficient aerosol-gas reactions would need to be in order to compete with atmospheric gas-phase reactions.

CHAPTER III

EXPERIMENTAL

Atom Recombination Rate Experiments: Wall Recombination

Description of Apparatus

Kinetic measurements for wall recombination were made using the fast-flow system shown schematically in Figure 1. Airco U.S.P. oxygen, minimum purity 99.6%, was used without further purification. The oxygen could be stored and used from a 5 l. bulb (B1) or used directly from the tank. B1 was used in conjunction with a mercury manometer (MAN1) for flow rate determinations. Oxygen was admitted to the flow tube through a brass shut-off valve (BV1) and a stainless steel needle valve (NV1) was employed to control system pressure and flow rate. The flow tube was pumped directly by a Welch Duo-Seal Model 1397B pump, having a pumping speed of 500 l./min. The flow tube had no traps or stopcocks. Early tests showed significant back diffusion of gases into the discharge region when traps and stopcocks were present.

A bank of pressure gauges was installed just below NV1. Two thermocouple gauges, TCG1 and TCG2 were used for

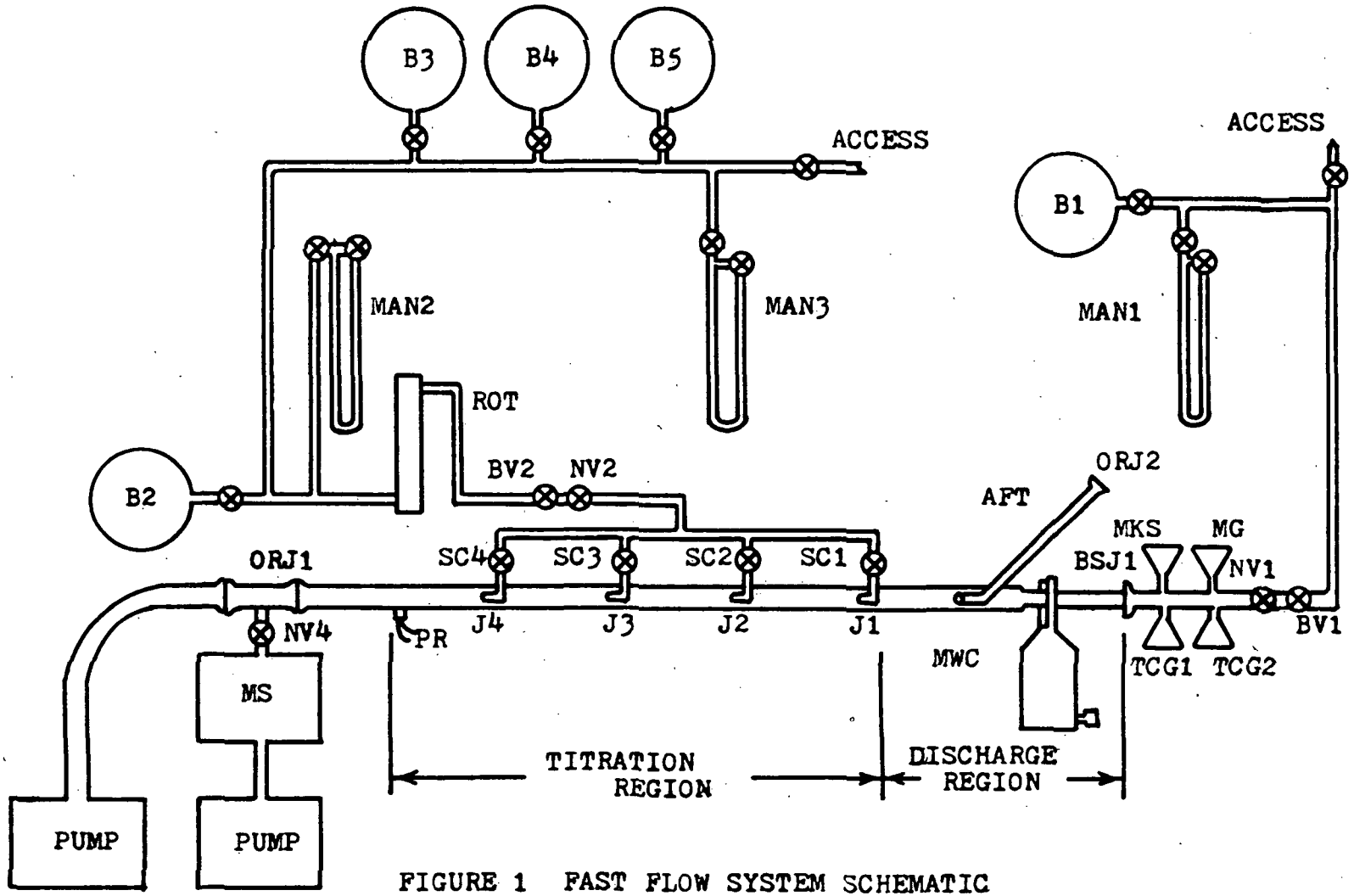

FIGURE 1 FAST FLOW SYSTEM SCHEMATIC

semi-quantitative measurements of system pressure. TCG1 (Hastings VT-45) had a range of 0.5-20 torr, and TCG2 (Hastings RV-8) had a range of 1-20 micron. The gauges were calibrated against a McLeod gauge (MG) Consolidated Vacuum Corporation. GM0100A, but changed calibration periodically. Pressure readings for actual runs were made with an MKS Baratron Pressure Meter Type 144 (MKS), referenced to pressure less than one micron.

The entire "reactor" portion of the flow tube was removable (for cleaning or coating) by use of a rubber O-ring joint, ORJ1, and a ball-and-socket joint, BSJ1. The joint BSJ1 was sealed with Apiezon W wax. The upper portion of the reactor was the discharge region made of 13 mm o.d. Pyrex glass. The microwave discharge cavity (MWC) could be placed anywhere along the 24 cm length of this tube.

Microwave power was generated with a Raytheon Microtherm unit, KV104 A, capable of 125 watts output and generally operated at 60 to 80% power. The generator was coupled by a coaxial cable to a movable cavity, Raytheon Model FC-7097 NBS Waveguide, which fit around the Pyrex tubing. An oxygen plasma was generated by adjusting the microwave power and then briefly discharging a Tesla coil near the cavity to initiate the plasma. A stream of air

was directed onto the discharge region to dissipate the heat of the plasma. The percent dissociation of the oxygen stream varied between 2 and 7%, computed on the basis of flow ratios.

The titration region made of 16 mm o.d. Pyrex tubing had four gas inlet jets, J1-J4, each centered in the flow tube. Each Pyrex jet had an opening of approximately 1 mm, and could be opened or closed with a teflon stopcock (SC1-SC4). The interjet distances were measured with a cathetometer, after clamping the flow reactor in a vertical position. The distances measured were as follow: J1 - J2, 10.15 cm; J2 - J3, 10.27 cm; J3 - J4, 10.00 cm. The measured distances had a precision of ±.01 cm.

A photoresistor (PR) was located about 20 cm downstream from J4. The circuit diagram for the custom-built detector is shown is Figure 2. The detector was based on a Clairex CL 502 photoresistor with peak response at 5150 Å. This wavelength was suitable since the chemiluminescense from the oxygen atom-nitrogen dioxide titration reaction was a continuum from 3700 to 9000 Å, with a maximum near 6500 Å (24). The photoresistor was taped to the outside of the flow tube with black tape. The flow tube itself was covered with black tape for a distance of about 20 cm on either side of the detector to exclude

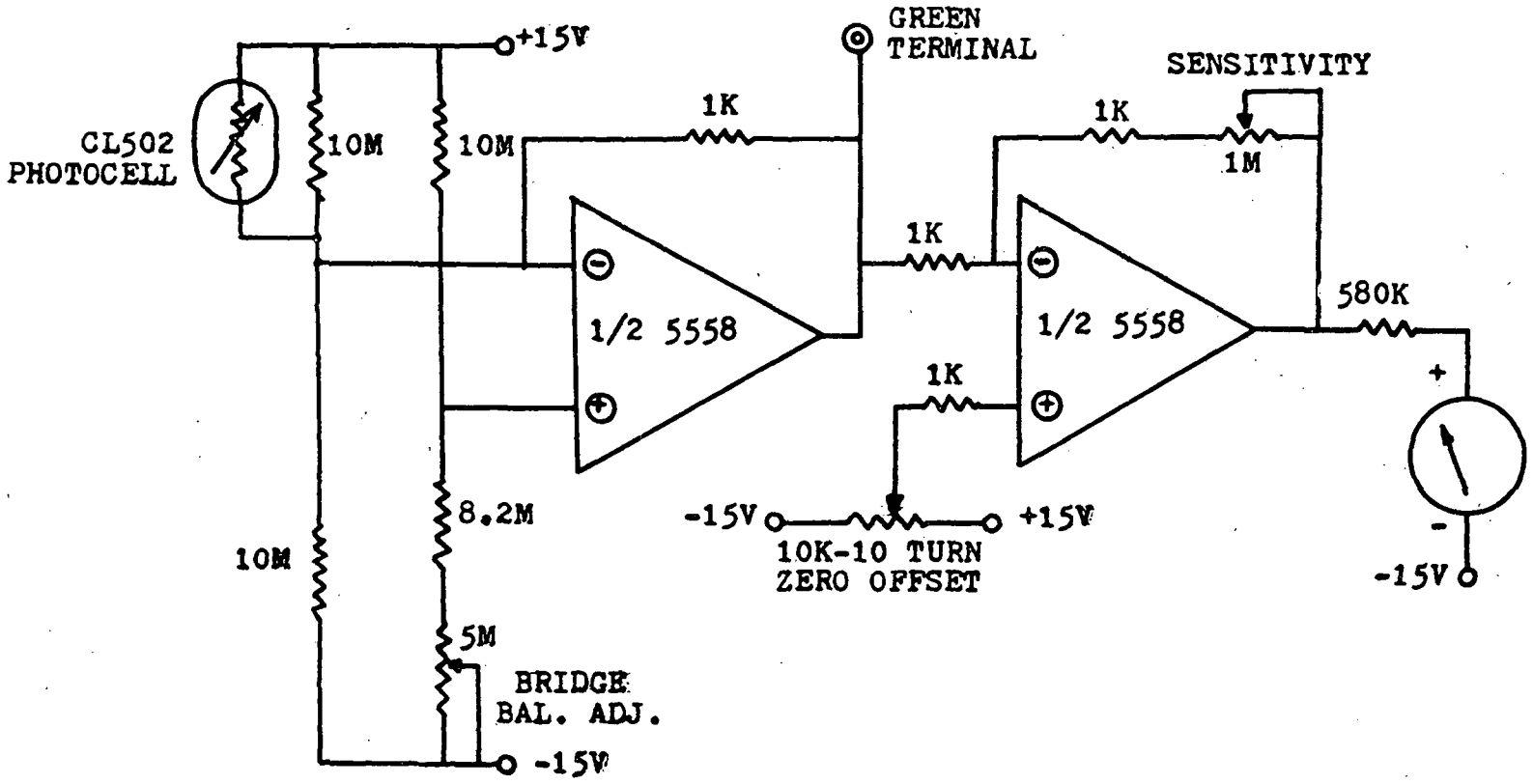

FIGURE 2 PHOTODETECTOR CIRCUIT DIAGRAM

extraneous light. The photodetector was part of a Wheatstone bridge. The bridge signal was amplified by a dual operational amplifier circuit and fed to a panel meter.

Oxygen atom concentrations were measured by the NO_2 chemiluminescent titration method of Kaufman (31). The titration system consisted of four 5 l. storage bulbs (B2-B5) for NO_2 (Matheson, 99.5% minimum purity) and the other components described below. A mercury manometer (MAN2) was used for flow rate determinations. A Matheson 622 PSM capillary rotameter with 610 tubes H501 and H194 was used to monitor NO_2 flow. A brass shut-off valve (BV2) and a stainless steel needle valve (NV2) were used to adjust NO_2 flow. The titration jets were described previously . The NO_2 pressure was maintained at 50 ± 1 torr to keep the N_2O_4 concentration low (32).

The NO_2 pressure could not be monitored continuously due to reactions between NO_2 and the manometer fluids. Mercury and hydrocarbon oils both reacted with NO_2 in a matter of minutes and NO_2 dissolved quickly in silicone oil. Thus, the pressure of NO_2 was checked periodically with a mercury manometer and the NO_2 in the manometer was pumped out immediately after measurement. This intermittent measurement technique worked satisfactorily since the large NO_2 storage capacity (approximately 20 l.) meant very slow NO_2 pressure changes from titration use.

Flow Rate Determinations

Oxygen: The volume of B1 was determined to be 5320 cm^3 by expansion of oxygen from a known volume. Operating pressures were set at 0.50, 0.80, 1.0, 1.3, and 1.5 torr. The flow rate at each of the five selected pressures was then calculated using the ideal gas law and the measured pressure drop in B1. Volume flow rates (cm^3/sec) were calculated from the relation

$$\Delta V/\Delta t = (\Delta P/\Delta t)(V)/P \qquad [36]$$

where $\Delta P/\Delta t$ (torr/sec) is the pressure drop in a known volume over a given time, V (cm^3) is the volume of B1, and P (torr) is the pressure maintained in the system by the flowing gas. Calculated O_2 volume flow rates are given in the last column of Table I.

Linear flow rates or linear flow velocities were calculated by dividing the volume flow rates by the cross sectional area of the flow tube. A cross sectional area of 1.45 cm^2 for the flow tube was based on a measured inside diameter of 13.6±.1 mm. The reciprocal of the linear flow velocity multiplied by the distance from J1 to each jet in turn, gave elapsed time values. The elapsed times were used in the kinetic calculations. O_2 linear flow velocities and elapsed times are summarized in Table II. An error analysis is given in Appendix I.

TABLE I

O_2 VOLUME FLOW RATES

Pressure (torr)	ΔP (torr)	Δt (sec)	$\Delta P/\Delta t$ (torr/sec)	$\Delta V/\Delta t$ (cm^3/sec)
0.50	80	1940	0.0412	439
0.80	82	1038	0.0790	526
1.0	120	826	0.1453	774
1.3	100	418	0.2392	988
1.5	100	318	0.3145	1115

TABLE II

O_2 LINEAR FLOW VELOCITIES AND ELAPSED TIMES

Pressure (torr)	Linear Flow Velocity (cm/sec)	Elapsed Time (10^{-2}sec) J1-J2	J1-J3	J1-J4
0.50	303	3.35	6.74	10.04
0.80	363	2.80	5.63	8.39
1.00	533	1.90	3.82	5.69
1.30	674	1.50	3.02	4.50
1.50	769	1.32	2.66	3.96

Nitrogen Dioxide: The determination of NO_2 flow rates and calibration of the NO_2 flowmeter were carried out in a manner similar to the O_2 flow rates. Flows were calculated in moles per second from the relation

$$\Delta n/\Delta t = (\Delta P/\Delta t)(V)/RT \qquad [37]$$

where V is the volume of B2 (5369 cm^3), R is the gas constant, and T is the absolute temperature. CO_2 was substituted for NO_2 in these calibration runs. This substitution was necessary because of the extreme reactivity of NO_2 towards mercury used in the manometer (MAN2) to measure pressure drops in B2 during flowmeter calibration. CO_2 was chosen since its molecular weight (44 g/mol) approximated that of NO_2 (46 g/mol). NO_2 flowmeter calibration results are given in Table III for Rotameter H501 and for Rotameter H194. An error analysis is given in Appendix I. A working or calibration curve was obtained by recording flowmeter reading (FMR) when the pressure in B2 was at 50 torr. The values of (a) flow rate, (b) log flow rate, and (c) the square of flow rate were plotted versus FMR. None of these plots gave a straight line. The most gradual curve was given by log flow rate versus FMR and this plot was used to estimate NO_2 flow rates during the kinetic runs. Flow calibration curves for H501 and H194 are shown in Figures 3 and 4. Similar working curves for O_2 were not necessary

TABLE III

NO_2 FLOWMETER CALIBRATION DATA

Flowmeter Tube H501

ΔP (torr)	Δt (sec)	$\Delta P/\Delta t$ (torr/sec)	$10^{-7}\Delta n/\Delta t$ (mol/sec)	FMR @ 50 torr (scale units)
4	4860	8.23×10^{-4}	2.3	19.0
6	5820	1.03×10^{-3}	2.9	21.0
10	2093	4.78×10^{-3}	14	55.0
10	1275	7.84×10^{-3}	22	62.5
10	1250	8.00×10^{-3}	23	69.0
10	551	1.81×10^{-2}	51	100.0
12	1490	8.05×10^{-3}	23	61.5
12	660	1.82×10^{-2}	51	99.5
10	920	1.09×10^{-2}	31	78.8

Flowmeter Tube H194

10	1787		16.1	42.0
10	1255		22.9	51.0
10	5746		5.01	18.9
10	3770		7.63	27.1
4	7775		1.48	10.0
6	5244		3.29	15.2
6	2676		6.45	24.5

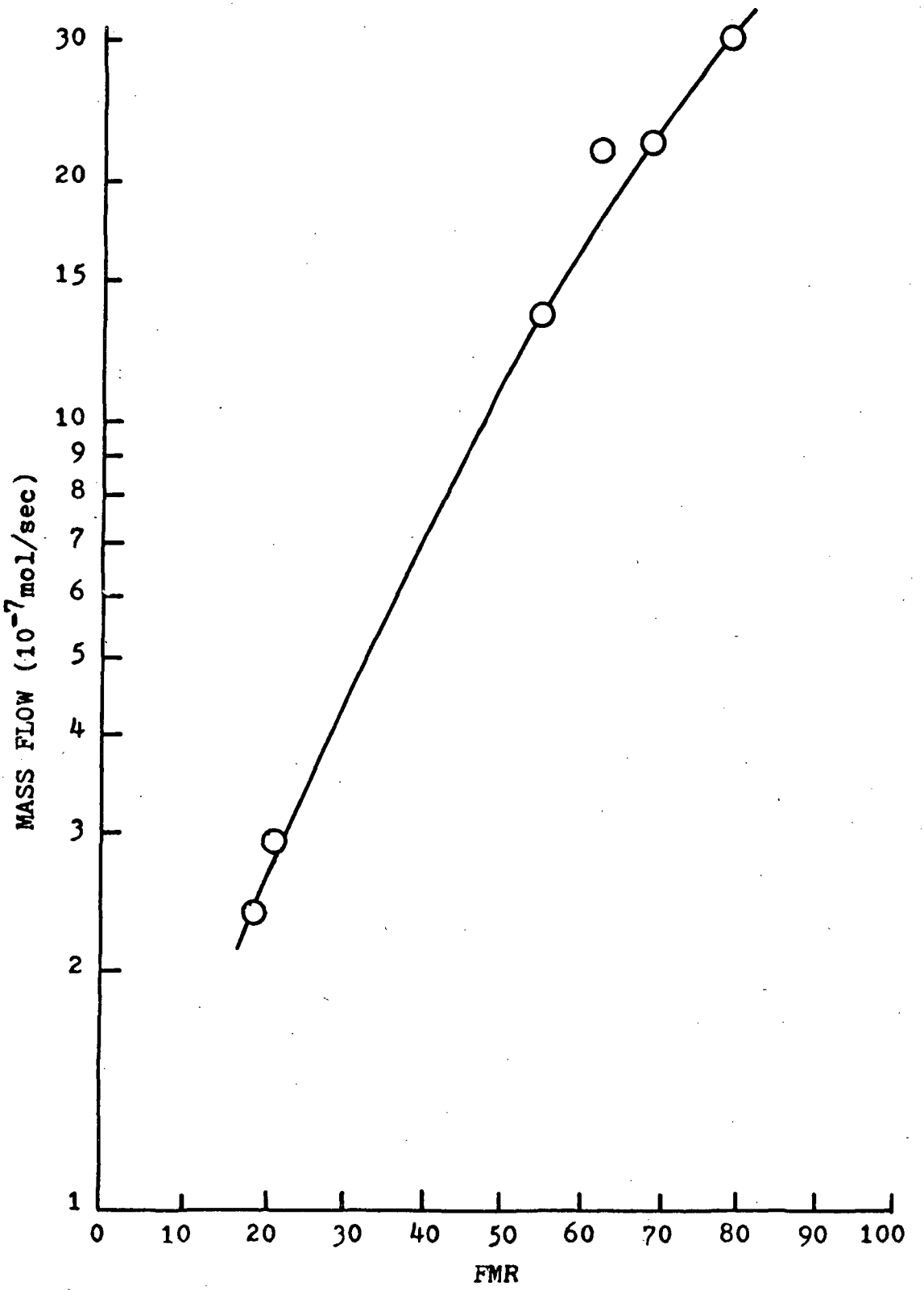

FIGURE 3 WORKING CURVE FOR NO_2 FLOWMETER H501

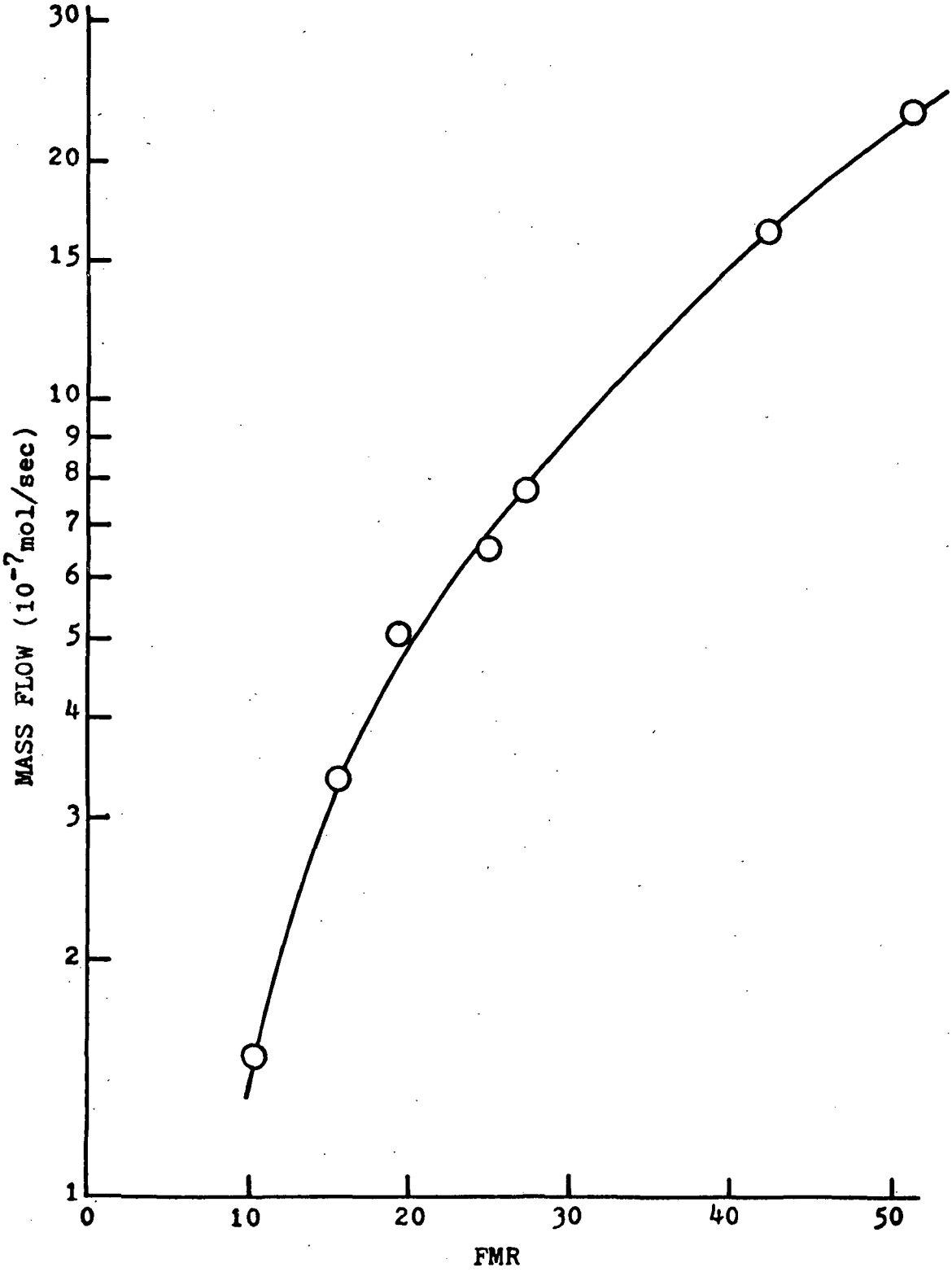

FIGURE 4 WORKING CURVE FOR NO_2 FLOWMETER H194

because runs were made at fixed pressures corresponding to previously calibrated flows.

Kinetics of Wall Recombination

Kinetic determinations were carried out as described below. First, the oxygen flow was adjusted by NV1 so that a constant pressure corresponding to one of those selected and characterized earlier was maintained. Next, the microwave unit was turned on and the percent power set to some figure above 50%. The discharge was then initiated. The microwave power was adjusted to the desired value for that run. Titrations were begun after a one to two minute warm-up period. SC1 was opened, and NV2 adjusted so that a maximum was noted on the photo-detector meter. The NO_2 rotameter reading was then recorded. The NO_2 flow at maximum intensity was recorded for each of the other jets in turn. This procedure was repeated two or more times for each of the selected pressures and for each of the wall treatments.

Wall Treatments

Clean: The term "clean wall treatment" means that the reactor tube had a nitric acid wash and a distilled water rinse. Concentrated HNO_3 was poured inside the tube and

the tube rotated so that the acid wet the entire surface. The acid was then drained from the tube. This was done three times each cleaning. Following the acid wash, distilled water was poured through the tube while the tube was rotated. Approximately one liter of water was used in this way for each rinse.

H_2SO_4 coated: The reactor was flushed profusely with distilled water and dried with a stream of dry nitrogen. Concentrated H_2SO_4 (Fisher Reagent A.C.S.) was poured in from the downstream end of the tube, and the reactor was rotated until all the area inside was seen to be wetted except the discharge region. This was repeated three times and the reactor was clamped in a vertical position until the excess acid drained. The reactor was positioned in the system and pumped down until a constant pressure was obtained before use. Once, during the H_2SO_4 runs, the flowmeter ball became lodged in one position. A dark brown liquid substance was observed to form in the reactor while using a high NO_2 flow rate and tapping to dislodge the ball. It was speculated that the observed substance was nitrosylbisulfate ($NOHSO_4$) formed from the reaction between H_2SO_4 and NO_2. The reactor was removed and recoated and no further brown liquid was observed during normal operation.

$(NH_4)_2SO_4$ coated: A saturated solution of $(NH_4)_2SO_4$ (Fisher Certified A.C.S.) was prepared in distilled water. The reactor was washed well with distilled water and the $(NH_4)_2SO_4$ solution poured in from the downstream end. The tube was rotated until all the wall area in the titration region was wet. The excess solution was poured out and more solution put in a total of three times. The reactor was clamped in a vertical position and oxygen gas passed through the tube until the tube was dry. A crystalline pattern was apparent on the walls but overall coverage was quite even. The discharge was operated for ten minutes to condition the reactor before the kinetic determinations were begun.

NH_4Cl coated: A concentrated solution of NH_4Cl (Fisher Certified A.C.S.) in distilled water was prepared and applied in the same fashion as the $(NH_4)_2SO_4$. However, droplets would form in the tube as the excess solution was drained, leading to spotty coverage. A dilute solution of NH_4Cl proved successful if dry nitrogen was passed through the tube while rotating some solution inside. A good coverage was obtained, showing a very fine crystalline pattern.

Atom Recombination Rate Experiments: Aerosol Interaction

Description of Apparatus

The system used for aerosol studies was basically the same as that used for wall recombination measurements. The titration region was modified to gain greater precision in the kinetic measurements. This involved a larger separation of the jets; the interjet distances were approximately doubled. The titration region was modified because the previous system gave a change in the logarithm of relative atom concentration (ln R) of about -0.2, a value not ideal for first-order kinetics determinations. Gardiner (82) recommends a change of 1.5 decades in concentration for first order studies, but this condition would require a flow tube length of four meters which was not feasible in this study. Other literature references were examined, and typical total changes in ln R were -0.6 (18) and -0.4 (37). The length of the titration region was doubled to give overall ln R values in the neighborhood of -0.4. The interjet distances were again measured with a cathetometer and found to be: J1-J2, 20.08 cm; J1-J3, 39.94 cm; and J1-J4, 59.54 cm. Table IV lists the new flow parameters and elapsed time calculations.

The elapsed time values in Table IV were used through 6/24/74, at which time a new pump was installed. Flow rates were redetermined and these values, used for all runs after 6/29/74, are shown in the last entry in Table IV.

A removable particle sampler was installed at ORJ1 (see Figure 1). The sampler was constructed of a 5 cm length of 16 mm o.d. Pyrex tubing, having an O-ring joint on each end. The upstream end had four indentations which supported the collector. The collector was cut from a plastic weighing bottle and had 15 holes of 2 mm diameter bored through it. The collector fit snugly into the sampler and could be removed for weighing. The tare weight of the collector was found by alternately washing with distilled water, placing in the reactor and pumping down to base pressure for about 10 min. The collector was removed and weighed on a Mettler Type H5 balance. This procedure was continued until several consecutive masses were the same. A tare weight of .1280 ± .0001 g was determined. Aerosols were collected by impaction on the collector for size, shape, and particle concentration determinations.

An aerosol generator was constructed, using gas phase reaction as the formation technique. Prototype designs were built to utilize the reaction of HCl(g) with NH_3(g) to form NH_4Cl(s) particles. No particles were obtained

TABLE IV

O_2 LINEAR FLOW VELOCITIES

AND ELAPSED TIMES - AEROSOL SYSTEM

Pressure (torr)	Linear Flow Velocity (cm/sec)	Elapsed Time (10^{-2}sec) J1-J2	J1-J3	J1-J4
0.50	303	6.63	13.18	19.65
0.80	363	5.54	11.02	16.43
1.0	533	3.75	7.47	11.13
1.3	674	2.97	5.91	8.81
1.5	769	2.61	5.19	7.74
1.5[a]	674	2.97	5.91	8.81

[a]These values used after 6-29-74

downstream using the first two designs shown in Figures 5a and 5b. Most of the solid seemed to form on the generator walls immediately below the inlet jets. This suggested a generator consisting of a large bulb so that reaction would take place before reaching a wall. The apparatus used to generate the NH_4Cl aerosol is shown in Figure 6. It consisted of a five liter Pyrex bulb with a carrier gas inlet, needle valve NV3, the aerosol stream outlet, a fitting for a thermocouple pressure gauge TCG3, and two removable Pyrex jets which reached to the center of the bulb. Supporting equipment included rotameters for the gases used: Matheson 622PS with a 601 tube for the NH_3 and Matheson 622PM with a 601 tube for the HCl. Matheson Anhyrdous NH_3, and Matheson Technical, 99.0% purity HCl were used without further purification.

For $(NH_4)_2SO_4$ aerosol generation, a custom built H_2SO_4 boiler replaced the HCl jet. Figure 7 shows the Pyrex boiler design. The standard taper joint and jet were made to fit the aerosol bulb, and H_2SO_4 vapor was produced by heating the concentrated acid (Fisher Reagent A.C.S.) with a 900 watt heater controlled by a Variac. The thermometer was used to monitor the temperature of the acid. Vapor pressure data for H_2SO_4 as a function of temperature are listed in Table V (83). Acid vapor flow was controlled

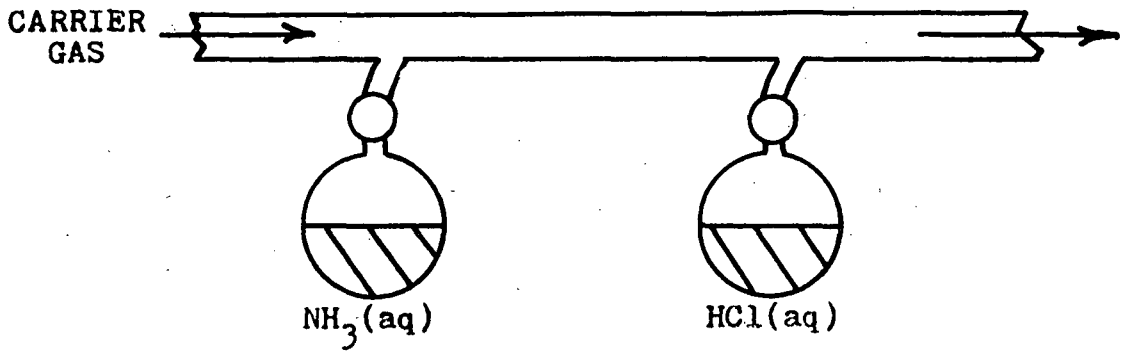

5a

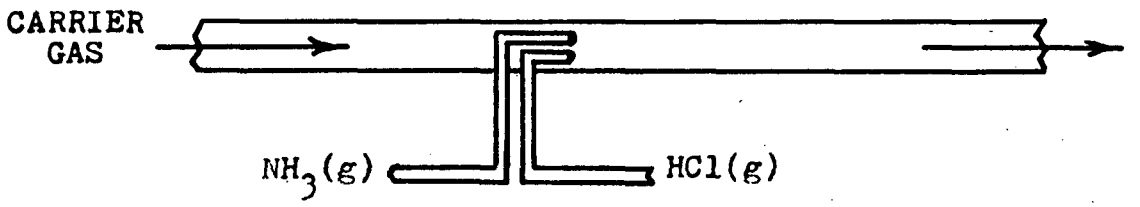

5b

FIGURE 5 PROTOTYPE AEROSOL GENERATORS

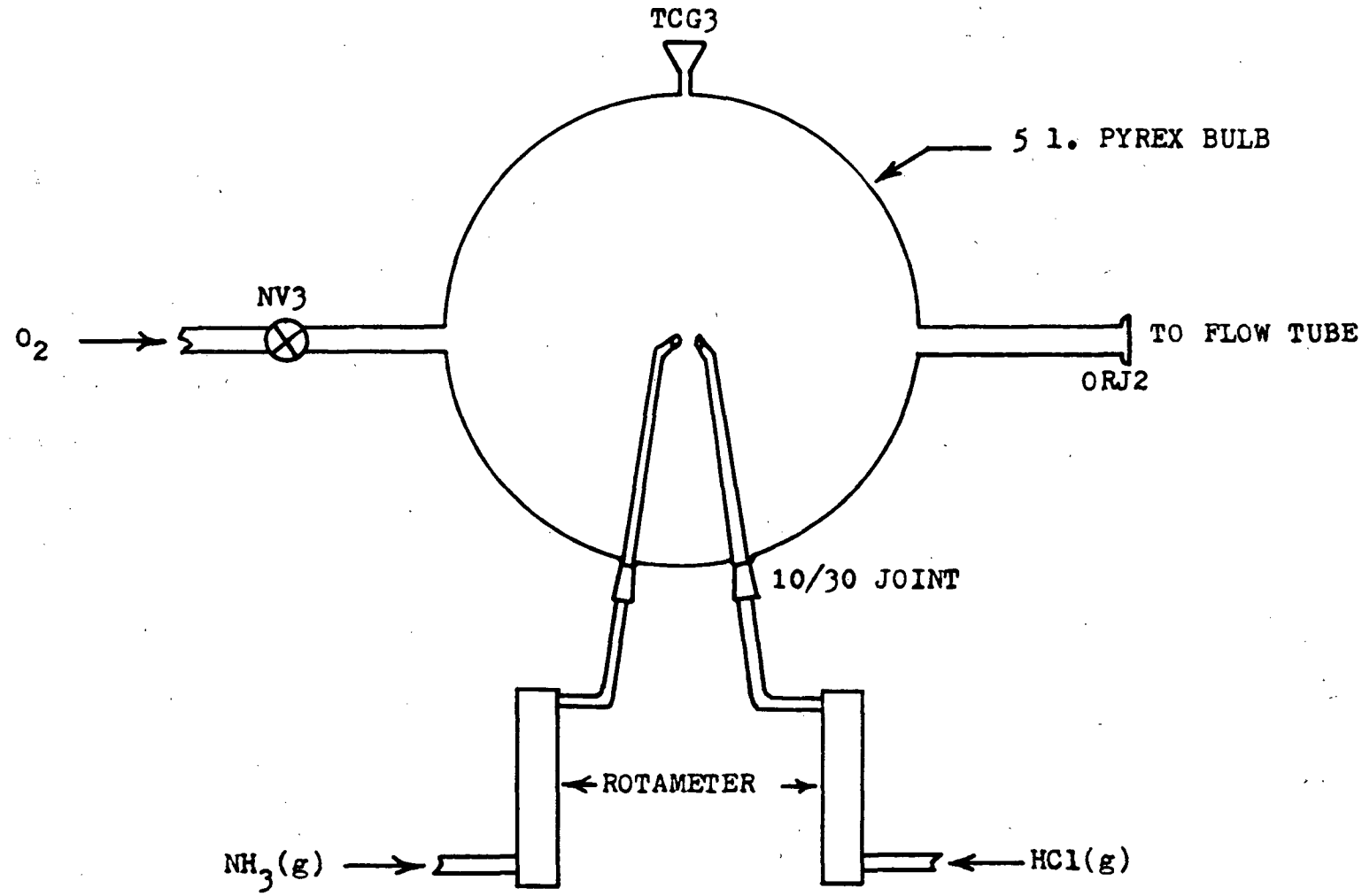

FIGURE 6 AEROSOL GENERATOR SCHEMATIC

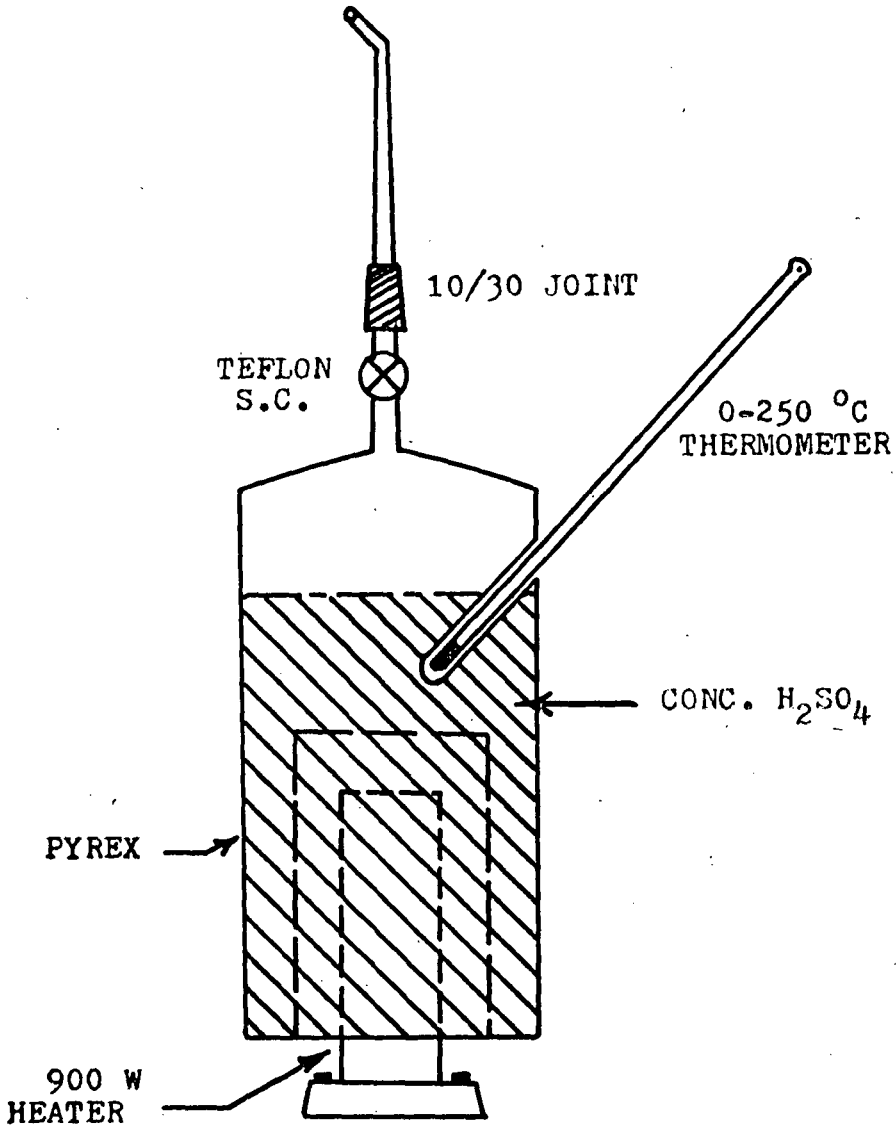

FIGURE 7 H_2SO_4 BOILER DIAGRAM

TABLE V

H_2SO_4 VAPOR PRESSURE DATA

Vapor Pressure (torr)	Temperature (°C)
0.001	60.3
0.01	71.8
0.02	81
0.03	86.7
0.04	92.0
0.05	94.6
0.06	97.4
0.07	100.1
0.08	101.5
0.09	102.9
0.10	105.8
0.20	116.1
0.30	123
0.40	129
0.50	132
0.60	137
0.70	139
0.80	140
0.90	142
1.0	145
2.0	158
3.0	167
4.0	174
5.0	178

by a teflon stopcock. The entire unit was wrapped with several layers of asbestos tape.

The discharge region of the flow tube was altered to accomodate the aerosol generator. The aerosol flow tube (AFT) was centered through the side of the reactor (Fig. 1). The generator exit was 10 cm above J1 to allow mixing before reaching the titration region. An O-ring joint, ORJ2, facilitated removal of the reactor (Fig. 6). An O-ring joint not shown was also placed between NV2 (Fig. 1) and the titration jets to aid removal of the reactor.

Aerosol Generation and Characterization

It was found for the NH_4Cl aerosol that the two reactant gases could be "titrated" by observing the pressure in the generator bulb or in the reactor system as the gases were mixed. When one gas, for example NH_3, was admitted to the system, the pressure would noticibly increase. When the other gas, HCl, was admitted, the pressure would drop to its original value. Further HCl addition increased the pressure. Systematic studies, made by setting the NH_3 flow at 14.5 (FMR) and varying the HCl flow showed that the lowest system pressure was obtained at an HCl FMR of 13.5. These two gas flowmeter settings were used for aerosol runs. The NH_4Cl aerosol

was characterized in the following three ways:

1. particle concentration,
2. particle shape, and
3. particle diameter.

The particle concentration was estimated by measuring the mass of the aerosol collected after varying collection times. Air, admitted to bring the flow system back to atmospheric pressure, was passed through a trap filled with Drierite. This minimized particle weight gain from absorbed moisture. The collector was then removed and immediately placed in a desiccator containing Drierite, prior to weighing on a Mettler balance. After weighing, the collector was rinsed copiously with distilled water and replaced in the system. Particle concentration values obtained from several runs are given in Table VI. A straight line was obtained when the mass of NH_4Cl collected was plotted versus collection time as shown in Figure 8. The slope of the line was 3.88 μg/sec. No particle entrainment (69) and a sticking coefficient of one was assumed. The particle flow was estimated by dividing the amount collected per unit time by the ratio of collector impaction area to tube area. Collector characteristics are listed in Table VII. A value of 5.29 μg/sec was calculated for the amount of NH_4Cl aerosol flowing past

TABLE VI

NH_4Cl AEROSOL PRODUCTION DATA

Date (1974)	Time	Condition When Run	Aerosol Exposure (min)	Mass (g)	Comments or Treatment
4-5	1135	aerosol	6.0	0.1295	washed after
4-9	-	clean	-	0.1289	looks dirty
4-10	AM	clean	-	0.1280	washed after
4-10	1400	clean	-	0.1280	washed after
4-11	1100	clean	-	0.1280	washed after
4-12	0920	aerosol	2.0	0.1285	washed after
4-15	0900	aerosol	4.0	0.1287	washed after
4-15	1530	clean	-	0.1280	washed after
4-15	1600	clean	-	0.1280	washed after
4-15	1625	aerosol	5.0	0.1290	washed after
4-16	0900	aerosol	8.0	0.1300^-	washed after
4-16	1000	aerosol	10.0	0.1300^+	washed after
7-8	0900	clean	-	0.1280	washed after
7-8	0915	clean	-	0.1280	washed after
7-8	0930	aerosol	6.0	0.1294	saved sample

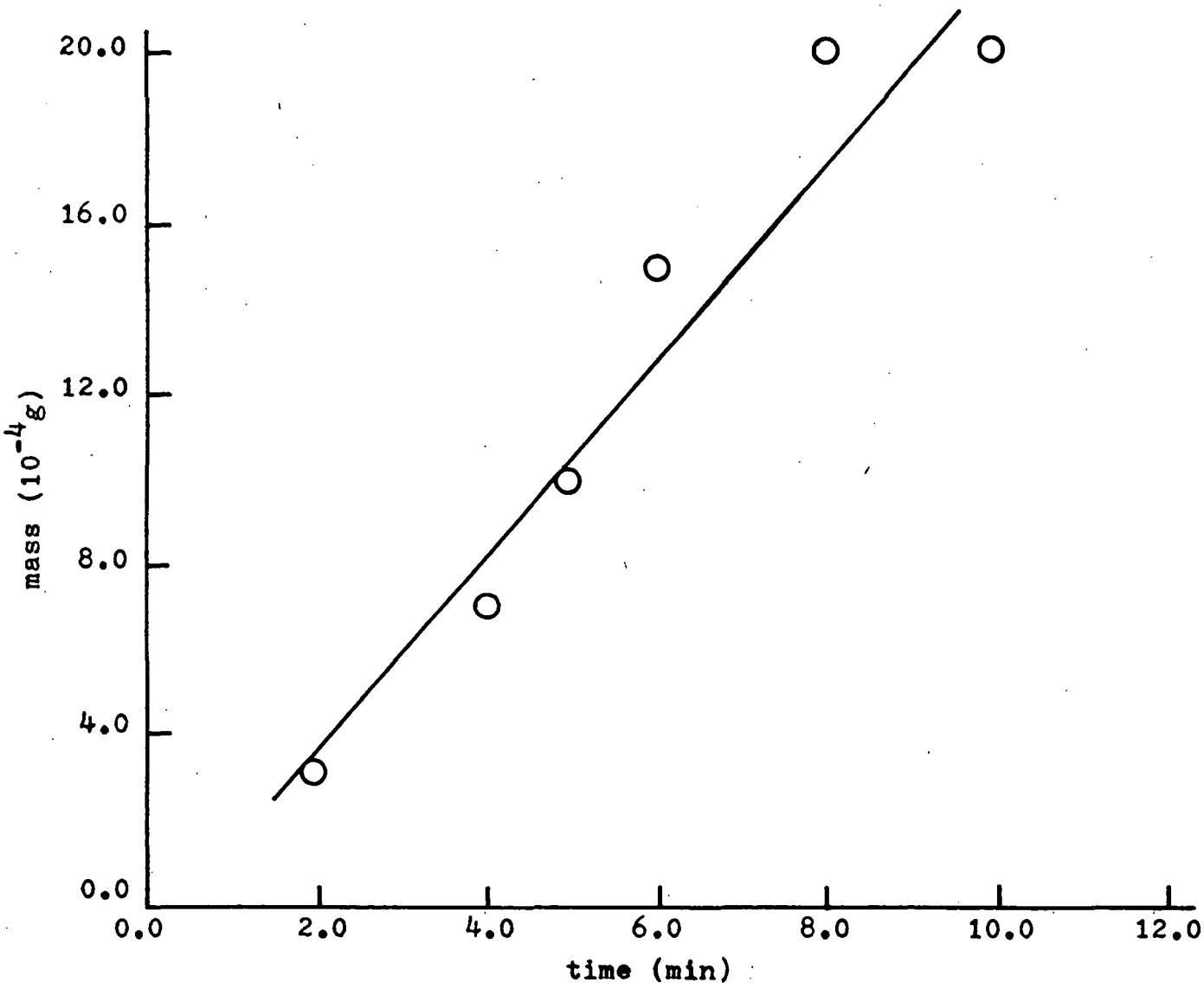

FIGURE 8 PLOT OF AEROSOL MASS COLLECTED VERSUS TIME

TABLE VII

AEROSOL COLLECTOR CHARACTERISTICS

Mean Diameter (mm)	15
Number of Holes	15
Hole Diameter (mm)	2
Total Collector Area (mm^2)	176.7
Area per Hole (mm^2)	3.1416
Total Hole Area (mm^2)	47.12
Collection Area (Total Area - Hole Area) (mm^2)	129.6
Ratio of Impaction Surface to Total Tube Area	0.733

a given point in the reactor. The oxygen pressure was set at 1.5 torr for the aerosol runs, corresponding to a gas volume flow rate of 1.115×10^{-3} m^3/sec. A particle concentration of 4.75×10^3 $\mu g/m^3$ was calculated from the ratio of mass collected per unit time to volume flow rate. The collected particles were examined using an Advanced Metals Research model 900 scanning electron microscope. Three different areas on the collector were examined, each at an 18X, 980X, and 4800X magnification. A typical photomicrograph can be seen in Figure 9, taken at 4800X. The particles are approximately spherical and are all about the same size. The mean particle diameter was estimated to be $1.6 \pm .2$ μm based on the 4800X photomicrograph.

The characterization of the $(NH_4)_2SO_4$ aerosol is included in Appendix IX.

Kinetic Determinations with Aerosol Present - NH_4Cl

All aerosol runs were performed at a system pressure of 1.5 torr. The constant pressure was attained by first adjusting NV1 (Fig. 1) so that the oxygen flowing through the discharge portion gave a system pressure of 1.0 torr; then NV3 (Fig. 6) was adjusted to give a total system pressure of 1.5 torr. Atom concentrations were measured in the same way as described above. For some runs, the aerosol flow was started first and then the oxygen plasma was initiated. For other runs, the aerosol and plasma

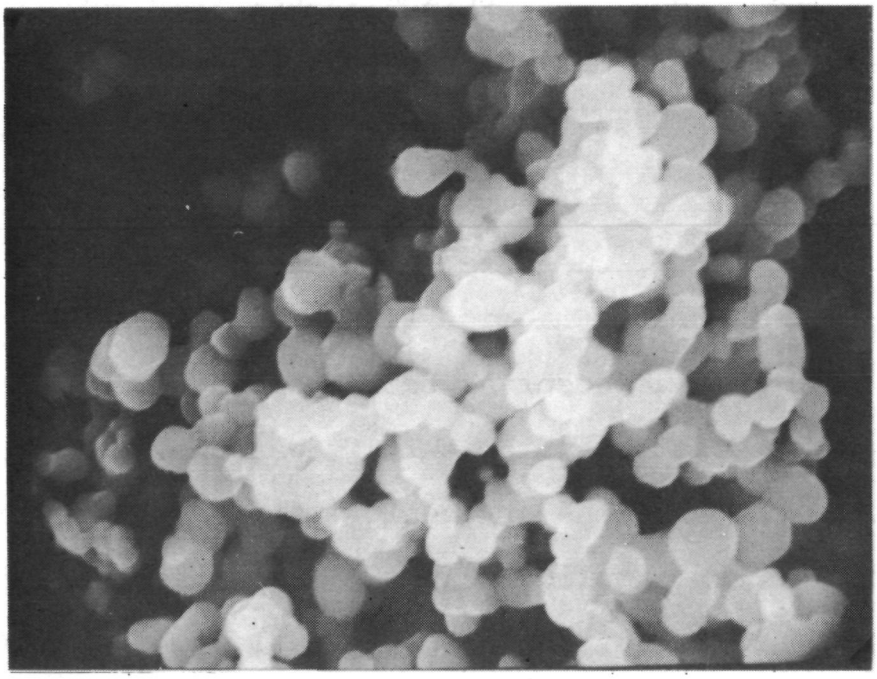

FIGURE 9

PHOTOMICROGRAPH OF NH_4Cl AEROSOL PARTICLES

were initiated simultaneously. For still other runs the plasma was started first and then the aerosol flow begun.

Aerosol runs were preceded by "pre-sol" runs and followed by "post-sol" runs to monitor changes in wall recombination. The effect of possible excess NH_3 or HCl on the oxygen disappearance kinetics was ascertained by allowing these gases to flow individually in the system. Flows equivalent to maximum possible excesses of NH_3 or HCl were used. These flows corresponded to a flowmeter reading of 1.0.

Product Analysis:

Ammonium Chloride Plus Atomic Oxygen

A reaction was observed between the NH_4Cl wall coating and O. Mass spectrometric analysis was chosen for product determination. In-line cryogenic trapping of products proved unsuccessful for sampling. An AEI MS-10 mass spectrometer (MS) was then installed as shown in Figure 1. The spectrometer inlet was attached by modifying the removable sampler. The first experimental conditions were to set the discharge in operation at one torr, with an NH_4Cl coating on the walls. Then the mass spectrometer leak needle valve NV4 was adjusted to give a MS system pressure of 6×10^{-6} torr. Chlorine (m/e = 35) was used as an indicator that products

were being sampled and no chlorine was found. The next experiment assumed that the product concentrations were too small to measure. Therefore several grams of NH_4Cl were piled in the reactor just below the discharge. Again no chlorine was found, using the same flow conditions.

The third experiment assumed a poor conductance through the mass spectrometer inlet tube. The MS and the MS ion gauge were turned off, and NV4 was opened fully for 2 minutes while the NH_4Cl - O reaction proceeded. NV4 was closed until the MS system pumped down, and then adjusted to give a sampling pressure of 6×10^{-6} torr. The MS was turned on and runs were carried out. This technique proved successful and was used for several runs. This sampling technique was also used with the discharge turned off and O_2 flowing in the NH_4Cl wall coated system.

ESCA: Reactor Wall Samples

ESCA was used to characterize the reactor wall surface in connection with wall recombination studies. An AEI ES 100 photoelectron spectrometer employing Al K_α radiation (1486.6 eV) was used to monitor the elements silicon, oxygen, sulfur, nitrogen, and carbon. Pyrex glass plates (8x5x1 mm) cut from large diameter tubing were treated in the same manner and order as the Pyrex reactor walls. Treatments for the samples were:

a. no treatment: used as obtained from glass shop;

b. HNO_3 wash, distilled H_2O rinse;

c. above treatment followed by coating with $(NH_4)_2SO_4$;

d. above treatments followed by an H_2O rinse and H_2SO_4 coating. This remained on the sample for 48 hours, then was rinsed off with distilled H_2O. The plate was HNO_3 washed and H_2O rinsed, and thus ready to run on ESCA.

An H_2SO_4 coated plate was not run in the ESCA. Specific spectrometer operating conditions are noted in the subsequent spectra.

CHAPTER IV

RESULTS AND DISCUSSION

Determination of k_{APP}

Any kinetic run yielded four data points. Each point consisted of the flow rate of NO_2 at maximum emission intensity measured as a function of distance in a flow tube. The flow tube distance was related to elapsed time of reaction through known flow rates. This data was taken to indicate the decrease in concentration of atomic oxygen with time in the confines of the flow tube reactor. A discussion of the errors in these values is found in Appendix I. Since, under the experimental conditions selected, the disappearance of oxygen atoms has been shown to follow first order kinetics (18), the data were treated as follows.

The NO_2 titrant flow at J1, measured in moles per second, was taken as equal to one-half the molar flow rate of atomic oxygen at $t = 0$, $[O]_0$. The flows at jets two through four $[O]_t$ were then compared to $[O]_0$ in a ratio $[O]_t/[O]_0$, hereafter referred to as R. Slopes of plots of the natural logarithm of R (ln R) versus elapsed time (t) were found by least squares analysis. This

least squares analysis was done by a Digital Equipment Corporation PDP-8/I computer using the FOCAL program shown in Appendix II. For many of the early runs, plots of ln R versus t, as illustrated by Figure 10, were drawn as a check on the linearity of the assumed first-order atom decay. As in Figure 10, good linear relations were obtained in nearly all cases. The negative of the slope of the straight line obtained was taken to be the rate constant for the first-order disappearance of atomic oxygen, and will be referred to hereafter as k_{APP}, the apparent rate constant.

Heterogeneous Wall Recombination

Values of $k_{APP}(sec^{-1})$ were determined at several pressures for clean Pyrex walls and walls coated with either H_2SO_4, $(NH_4)_2SO_4$, or NH_4Cl. The data for the first three systems are given in Appendixes III-IV. An average value of k_{APP} at a given pressure was calculated using least squares analysis, by including all the data taken at that pressure. The results for one set of runs for each system are shown in Table VIII. For a given pressure and wall treatment, the calculated value of k_{APP} is listed with an error band of one standard deviation. The numbers in parenthesis indicate the number of separate determinations which were made to obtain the tabulated value of

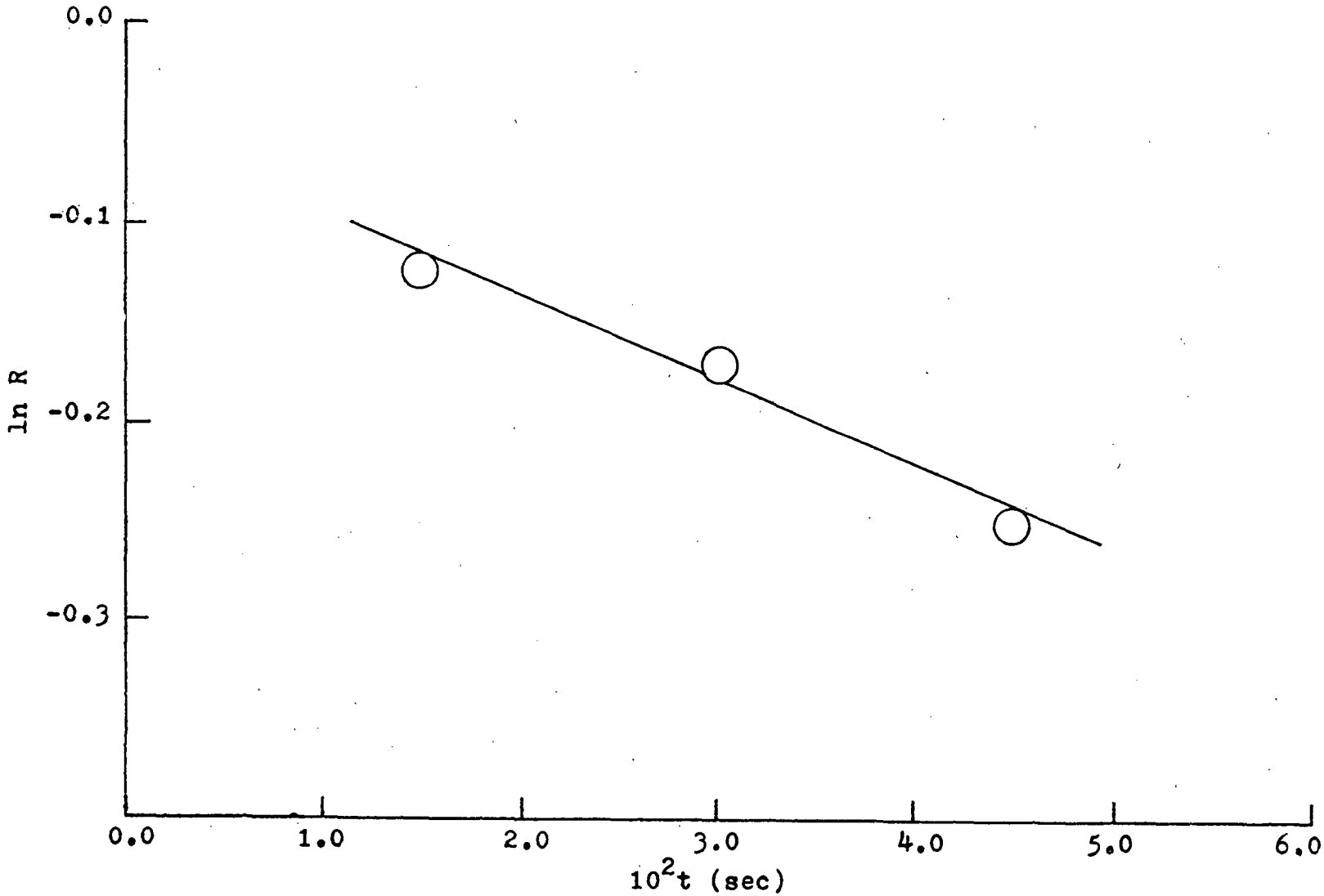

FIGURE 10 TYPICAL FIRST ORDER ATOM DECAY PLOT

TABLE VIII

CALCULATED VALUES OF k_{APP}

Pressure (torr)	k_{APP} (sec^{-1}) Clean[a]	H_2SO_4[b]	$(NH_4)_2SO_4$[c]
0.5	-	0.96±.16 (5)	1.15±.14 (6)
0.8	2.87±.23 (3)	1.08±.17 (4)	1.18±.15 (6)
1.0	2.93±.11 (3)	1.09±.31 (6)	1.24±.18 (4)
1.3	3.72±.40 (3)	1.18±.22 (3)	1.93±.56 (3)
1.5	4.14±.53 (3)	-	-

[a]Clean wall data taken on 6-4-74

[b]H_2SO_4 data taken 9-14-73 through 9-17-73

[c]$(NH_4)_2SO_4$ data taken 9-10-73 through 9-11-73

k_{APP}. Four other sets of runs were made for the clean wall. The results are not shown in Table VIII but are reflected in the value shown in Table IX. Kaufman (18) has stated that values of k_{APP} range between 1 and 5 sec^{-1} for a clean Pyrex wall system. The present data is seen to fall in this range. The value of k_{APP} could not be measured with an NH_4Cl wall coating. When measurements were attempted in the usual way, no glow whatsoever could be detected at J1. As atomic oxygen was generated, the NH_4Cl coating was progressively removed from the tube, beginning at the end nearest the discharge. The flow tube felt hotter in the area where NH_4Cl was disappearing. The coating did not disappear when O_2 was flowing with the discharge turned off. This indicated negligible reaction of $NH_4Cl(s)$ with O_2 and negligible sublimation of $NH_4Cl(s)$. It was assumed that a very fast exothermic reaction was taking place between NH_4Cl and atomic oxygen. This is entirely different from wall catalysed recombination and is therefore omitted from this discussion. The results of a product analysis of this reaction are given below.

Values of k_{APP} were resolved into component rate constants by assuming that wall recombination was the only unimolecular mode of atom recombination, and that

any competing gas-phase reactions were termolecular and dependent on the square of the oxygen molecule concentration. Thus, a plot of k_{APP} versus oxygen pressure squared (equation [14]) was assumed to yield a y-intercept equal to the wall recombination rate constant, k_{WALL}. The linearity of this plot should give an indication of whether the assumptions were valid. The data from Table VIII were plotted with error bars of one standard deviation as shown in Figure 11. The resulting plots showed linear relationships over the pressure ranges used. Least squares analysis provided the value of k_{WALL} (y-intercept) and its error, the error indicated to one standard deviation as calculated in Appendix I. Values of k_{WALL} thus obtained were then converted to recombination efficiency, γ, by equation [26]:

$$\gamma = k_{WALL}\, d/\bar{v} \qquad [26]$$

where d = 1.36 cm, and $\bar{v} = (8RT/\pi M)^{\frac{1}{2}}$. Using T = 300 °K and M = 16 g/mole, a value of $\bar{v} = 6.3 \times 10^4$ cm/sec was calculated. This gave the relationship

$$\gamma\,(\text{sec}) = 2.16 \times 10^{-5}\, k_{WALL}.$$

Calculated values for k_{WALL} and γ are listed in columns 2 and 3 in Table IX for each wall treatment shown in column 1. The clean wall values represent an average of the results of five separate sets of runs. Values calculated for γ are compared to some literature values in column 4 of

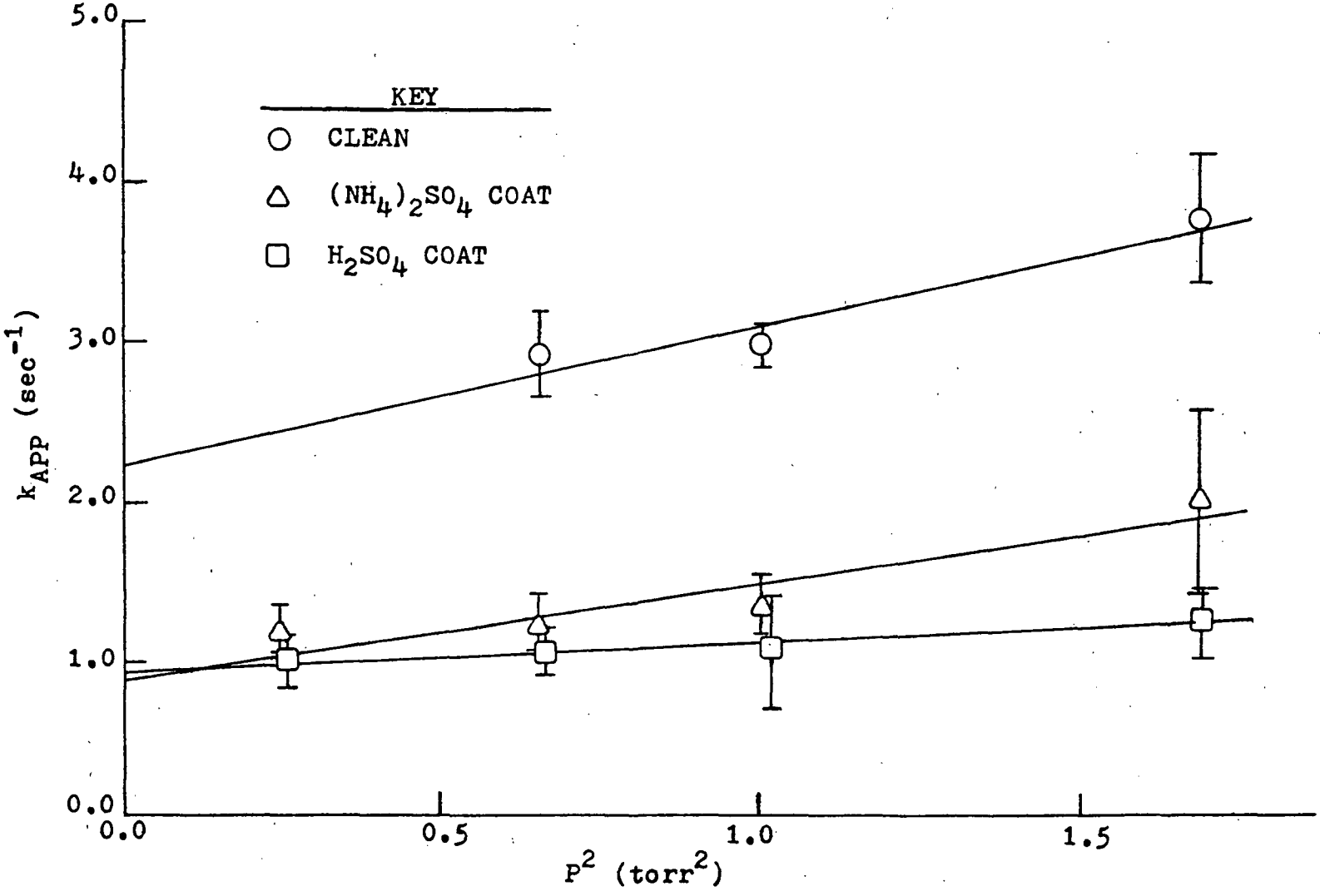

FIGURE 11 PLOT FOR RESOLUTION OF k_{APP}

TABLE IX

CALCULATED VALUES OF k_{WALL} AND γ
FOR EACH WALL TREATMENT

Wall Treatment	k_{WALL} (sec^{-1})	$10^5\gamma$	$10^5\gamma$ (Reference)	
Clean Pyrex	2.3±.7	4.97±1.5	2	(32)
			3.1-4.5	(84)
			5.4-6.8	(48)
H_2SO_4	0.95±.03	2.05±.06	2.3	(48)
$(NH_4)_2SO_4$	0.88±.18	1.90±.39	-	-

Table IX. The value of γ on clean Pyrex and for H_2SO_4 coated wall is seen to be in good agreement with reported values. The value of γ on $(NH_4)_2SO_4$ coated wall is the first reported value for this coating. This is surprising since $(NH_4)_2SO_4$ aerosol is prevalent in the stratosphere. It can be seen that H_2SO_4 significantly lowers γ and has been widely used as a wall coating to prolong atomic oxygen and ozone lifetimes (18, 48). The present work indicates that $(NH_4)_2SO_4$ may lower γ as much as or more that H_2SO_4, and thus suggests its use as an effective and easily handled wall treatment.

Homogeneous Gas Phase Recombination

Equation [15] was also used to calculate values of k_{GAS}, even though the gas phase oxygen recombination mechanism was unknown. Equation [15] was assumed valid and k_{GAS} was calculated by taking one-half of the slope of a k_{APP} versus pressure squared plot. Five sets of runs in a "clean" system gave a mean value of k_{GAS} equal to $1.46 \pm .61 \times 10^8$ l^2/mol^2 sec. This value is compared to literature values in Table X. Column one gives the value of k_{GAS}, while column two gives the author and reference number for that value. The most recent value of k_{GAS} was reported by Davis and Garvin

TABLE X

COMPARISON OF k_{GAS} VALUES

$10^{-8} k_{GAS}$ ($l.^2/mol^2 sec$)	Author	Year	Reference
0.6-2	Kaufman	1961	(18)
2.43	Johnston	1968	(85)
3.08	Mulcahy and Williams	1968	(85)
0.45	Francis	1969	(85)
2.31	Stuhl and Niki	1971	(85)
2.23	Davis and Garvin	1973	(85)
1.46	This study		

but was determined using a different method (flash-photolysis) from the method used in this study. The values reported by Kaufman and by Francis were obtained using discharge-flow apparatus and agreement is quite good between their values and the k_{GAS} value determined in this study. A method like flash-photolysis eliminates several uncertainties, such as wall factors, in measurements of k_{GAS}. From the information in Table X, it does appear that discharge-flow values of k_{GAS} tend to be somewhat lower, although not unreasonably more so than values found by more preferred (85) methods.

Kinetic Determinations with NH_4Cl Aerosol Present

Data for the NH_4Cl aerosol runs are given in Appendix VII. The value of k_{APP} was calculated for each consecutive kinetic run so that changes in the system would be more apparent.

When the aerosol was started before initiation of the plasma, the ensuing values of k_{APP} were quite large. For some of these runs, no glow was detected at jets past J1. This indicated a very rapid disappearance of oxygen atoms, and k_{APP} was unmeasurable. It was observed in these cases that aerosol generation resulted in the deposition

of particles onto the backs of the titration jets. Oxygen atom flow removed these particles in about 3 min. or less. This was determined by continuously monitoring the atom concentration at one jet (usually J4) until the concentration value stabilized. During simultaneous aerosol and plasma generation, it was observed that particles were removed faster than they were deposited. When initiating the plasma first, then beginning the aerosol flow, no build-up of particles was observed. Values of k_{APP} were measurable in this case and on the same order of magnitude as those measured earlier for clean wall recombination. It was therefore assumed that k_{APP} values calculated on the basis of the latter method gave the most accurate results for estimation of the effect of the aerosol on atom disappearance. This method was assumed to minimize the effect of loss of oxygen atoms to reaction with excess NH_4Cl on the walls. k_{APP} values for no aerosol present were determined before and after aerosol runs. It was found that k_{APP} for post-sol runs was usually significantly lower than k_{APP} for pre-sol runs. It was assumed that some species generated during the atom-aerosol run was poisoning (deactivating) the wall toward atom recombination. It was also assumed that this poisoned wall condition was effective during the aerosol run. The rate constant

for the disappearance of oxygen as influenced by the aerosol, k_{AERO}, was thus assumed to be equal to the difference in k_{APP} values for two consecutive runs, one run with aerosol flowing ($k_{APP}^{AEROSOL}$) and the other run with no aerosol ($k_{APP}^{POST-SOL}$):

$$k_{AERO} = k_{APP}^{AEROSOL} - k_{APP}^{POST-SOL}$$

k_{APP} values obtained while operating with the aforementioned conditions are summarized in Table XI. Column 1 gives the numbers of the aerosol and post-sol runs. The values of k_{APP} for the aerosol and post-sol runs are given in columns 2 and 3, and the difference, k_{AERO}, is listed in column 4. The mean value calculated for k_{AERO} is $2.7 \pm .5$ sec^{-1} to one standard deviation. This value could not be compared as it was the first such reported value. The value of k_{AERO} reflects primarily the rate of reaction between atomic oxygen and NH_4Cl. Although catalytic oxygen recombination may be taking place on the particles' surfaces, it would seem to contribute only slightly to atom disappearance because of the rapid exothermic reaction known to occur between these species.

It was of interest to compare the value of k_{AERO} to a calculated value of the rate constant upper limit for an aerosol-gas reaction. The model of Judeikis and

TABLE XI

SUMMARY OF AEROSOL AND POST-SOL k_{APP} VALUES WITH CALCULATED VALUES OF k_{AERO}

Run Number	$k_{APP}^{AEROSOL}$ (sec^{-1})	$k_{APP}^{POST-SOL}$ (sec^{-1})	k_{AERO} (sec^{-1})
7-2-11A, 12	2.42	0.56	1.86
7-3-10A, 11	4.18	0.57	3.61
7-6-7A, 8	1.43	0.00	1.43
7-6-9A, 10	3.21	0.00	3.21
7-6-11A, 12	1.43	0.00	1.43
7-6-17A, 18	4.77	0.00	4.77

Siegel (76) estimates the upper limit for the reaction or adsorption rate based on the number of collisions with the surface of an aerosol particle. Equation [38], was used to calculate the value of k_{CALC}, the upper limit to the rate of reaction:

$$k_{CALC} = (RT/2\pi M_G)^{\frac{1}{2}}(3\gamma W/\rho r_m). \qquad [38]$$

For $W = 4.75 \times 10^{-6}$ kg/m^3, $\rho = 1500$ kg/m^3, $r_m = 8 \times 10^{-5}$ cm, $M_G = 16$ g/mol, $\gamma = 2$, and $T = 300$ °C, the value of k_{CALC} is 3.74 sec^{-1}. This value is very close to the value of $2.7 \pm .5$ sec^{-1} obtained for k_{AERO} (Table XI). Although this agreement may be fortuitous, it indicates that this model may have merit and should be studied further. If indeed the model were adequate for describing the NH_4Cl-O system, the close agreement between the measured and the calculated rates would indicate a very high probability of reaction upon collision of an oxygen atom with an NH_4Cl particle.

The effects of possible excess flows of NH_3 or HCl from the aerosol generation reaction were shown to be negligible. Table XII lists the k_{APP} values obtained from the data in Appendix VIII. The k_{APP} values, determined while admitting excess reactants, show k_{APP} to be the same or slightly lower in the case of either reactant. In addition, the post-run value of k_{APP} returned to pre-run value in most cases (Table XII) which was not observed

TABLE XII

EFFECT OF EXCESS AMOUNTS OF NH_3 OR HCl ON k_{APP}

Date	Gas Added:FMR	k_{APP} (sec^{-1}) Pre-run	Added Gas	Post-run
6-18-74	NH_3:1.0	1.8	1.1	1.8
6-19-74	NH_3:1.0	4.8	2.8	3.4
6-20-74	NH_3:1.0	4.0	3.1	4.0
6-21-74	HCl:1.0	1.65	1.38	1.65
6-21-74	HCl:1.0	1.65	1.65	1.63

when the aerosol was present.

Only qualitative kinetic results were obtained with the $(NH_4)_2SO_4$ aerosol. The results, however, are included in Appendix IX due to the paucity of even qualitative data in the atom-aerosol interaction area.

Product Analysis: NH_4Cl + O

As noted above, a reaction was observed to occur between atomic oxygen and NH_4Cl. No report of this reaction was found in the literature. It was therefore of interest to determine the reaction products. Mass spectrometric analysis of the products of the reaction NH_4Cl + O showed increases in the m/e values equal to 14, 17, 18, 26, 30, 35, 36, 37, and 38. These m/e values were assigned to the species NH^+ and/or OH^+, H_2O^+, NO^+, and HCl^+. To determine whether m/e = 17 was representing OH^+ or NH_3^+, consecutive runs were made with the plasma off, then on. With the plasma on, m/e = 17 increased by a factor of 1.63, while m/e = 18 increased by a factor of 1.17. It was therefore assumed that NH_3, in addition to H_2O, was being formed. The reaction products between atomic oxygen and NH_4Cl(s) were thus concluded to be NH_3, H_2O, NO, and HCl.

ESCA: Reactor Wall Samples

ESCA has been shown to be a useful technique for surface analysis (86). ESCA was used in the present study to see if changes in the calculated recombination rates of

atomic oxygen could be correlated with changes in surface composition. ESCA spectra obtained for the Pyrex samples coated with $(NH_4)_2SO_4$ are shown in Figures 12 through 16, for Si, O, N, S, and C respectively. Binding energies for these elements, taken from the ESCA spectra are listed in Table XIII. The carbon 1s electron energy was used to calibrate the spectra. The energy was taken to be 285.0 eV (87) and all binding energies were normalized to this energy. The binding energy of Si is quite constant, indicative of good reproducibility. The shift of -0.9 eV in the binding energy of O for the $(NH_4)_2SO_4$ coating indicates a different bonding state of O in the coating and the untreated glass. The only significant S peak was found in the $(NH_4)_2SO_4$ coating. Marginal N peaks were observed for both HNO_3 washed and after full treatment. The shift of +1.7 eV in binding energy of N for the $(NH_4)_2SO_4$ coating again points to a different bonding state of N in the coating and the untreated Pyrex.

Table XIV summarizes the results of an intensity analysis of the ESCA spectra. The difference between the maximum and minimum counts is Δ. Ratios of Δ to the minimum number of counts per scan are listed for each element in Table XIV. The Si peak in Pyrex was strong except for the $(NH_4)_2SO_4$ coated glass. The

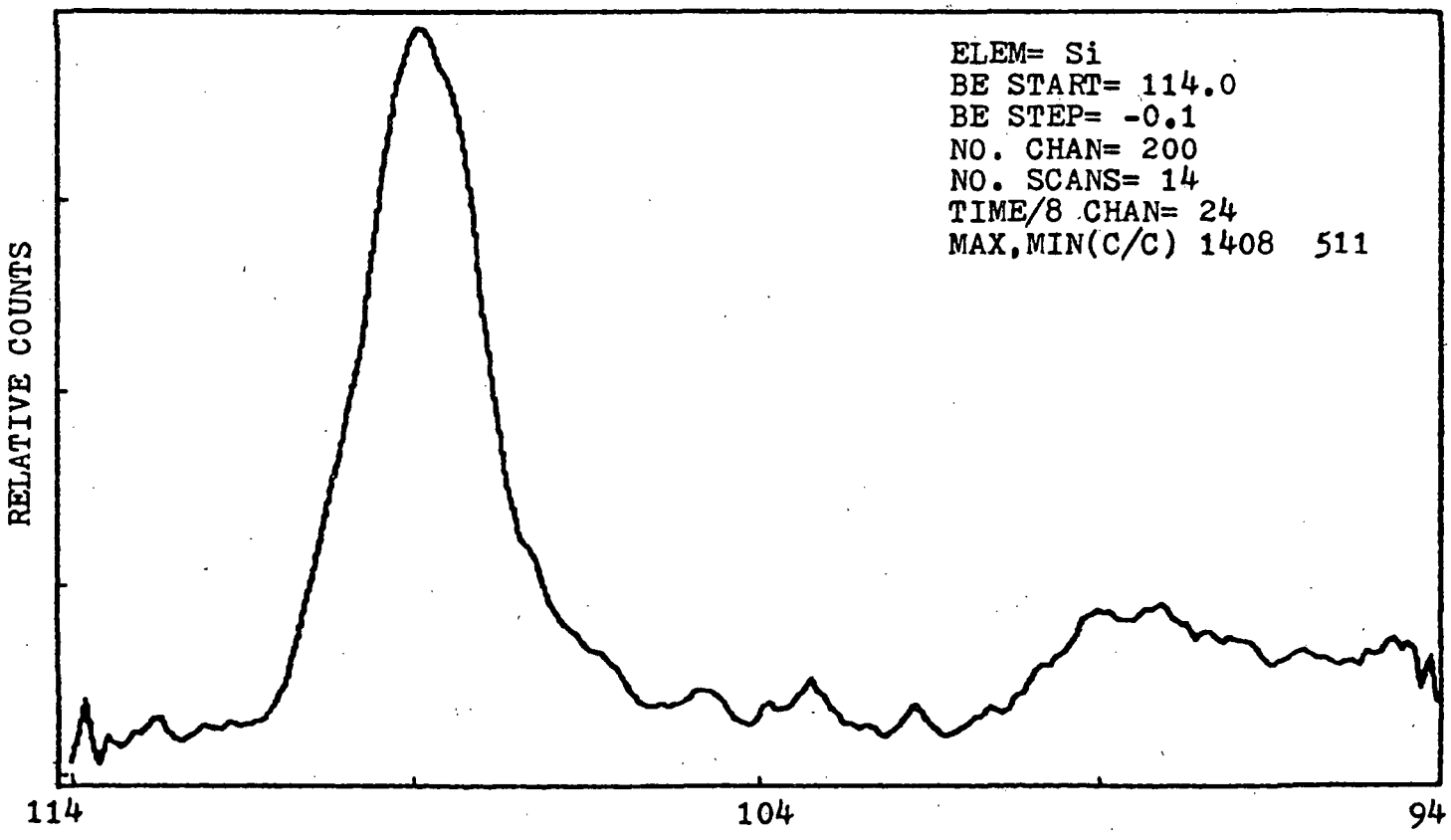

FIGURE 12 ESCA SPECTRUM OF Si IN $(NH_4)_2SO_4$ COATED PYREX

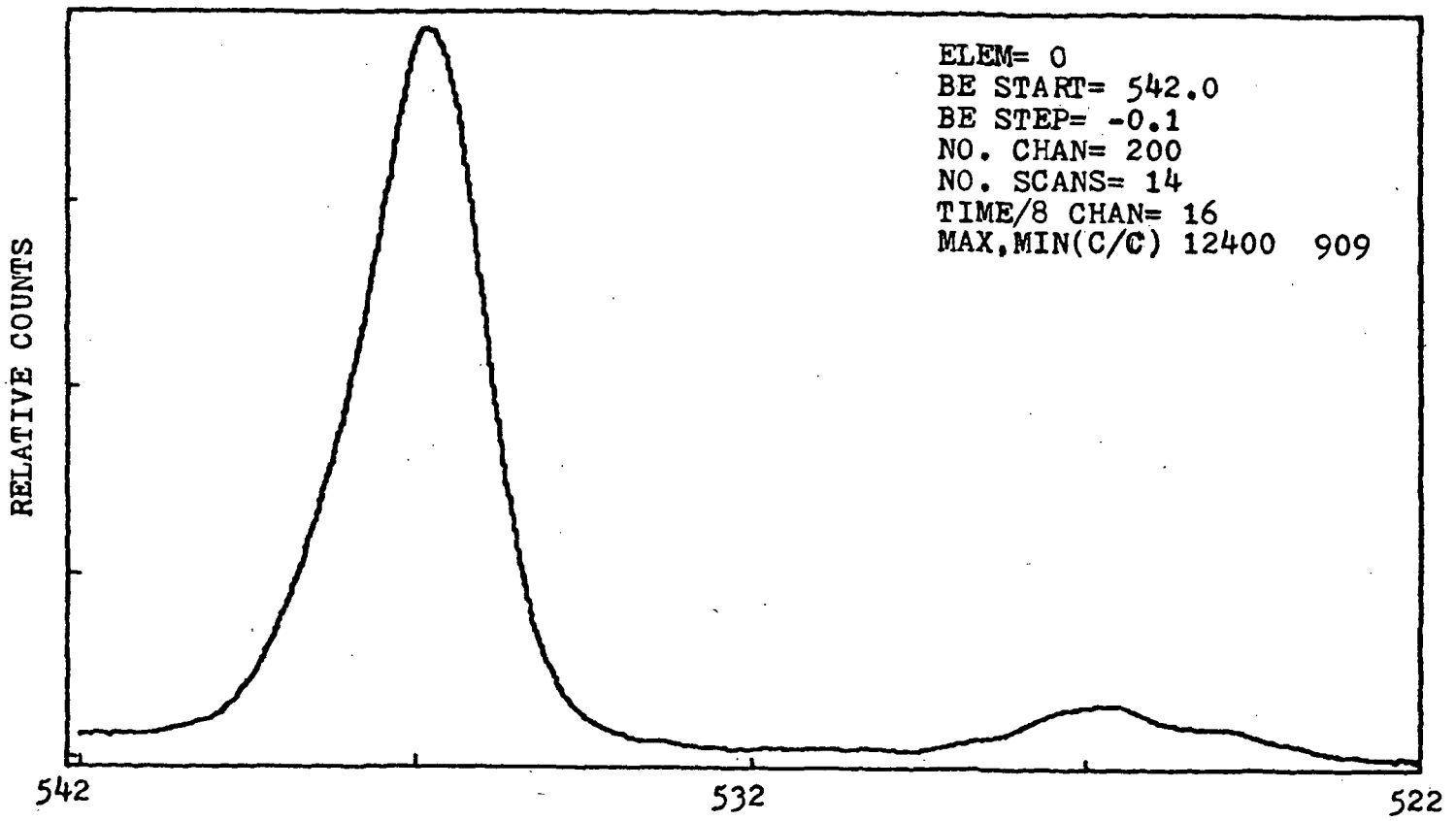

FIGURE 13 ESCA SPECTRUM OF O IN $(NH_4)_2SO_4$ COATED PYREX

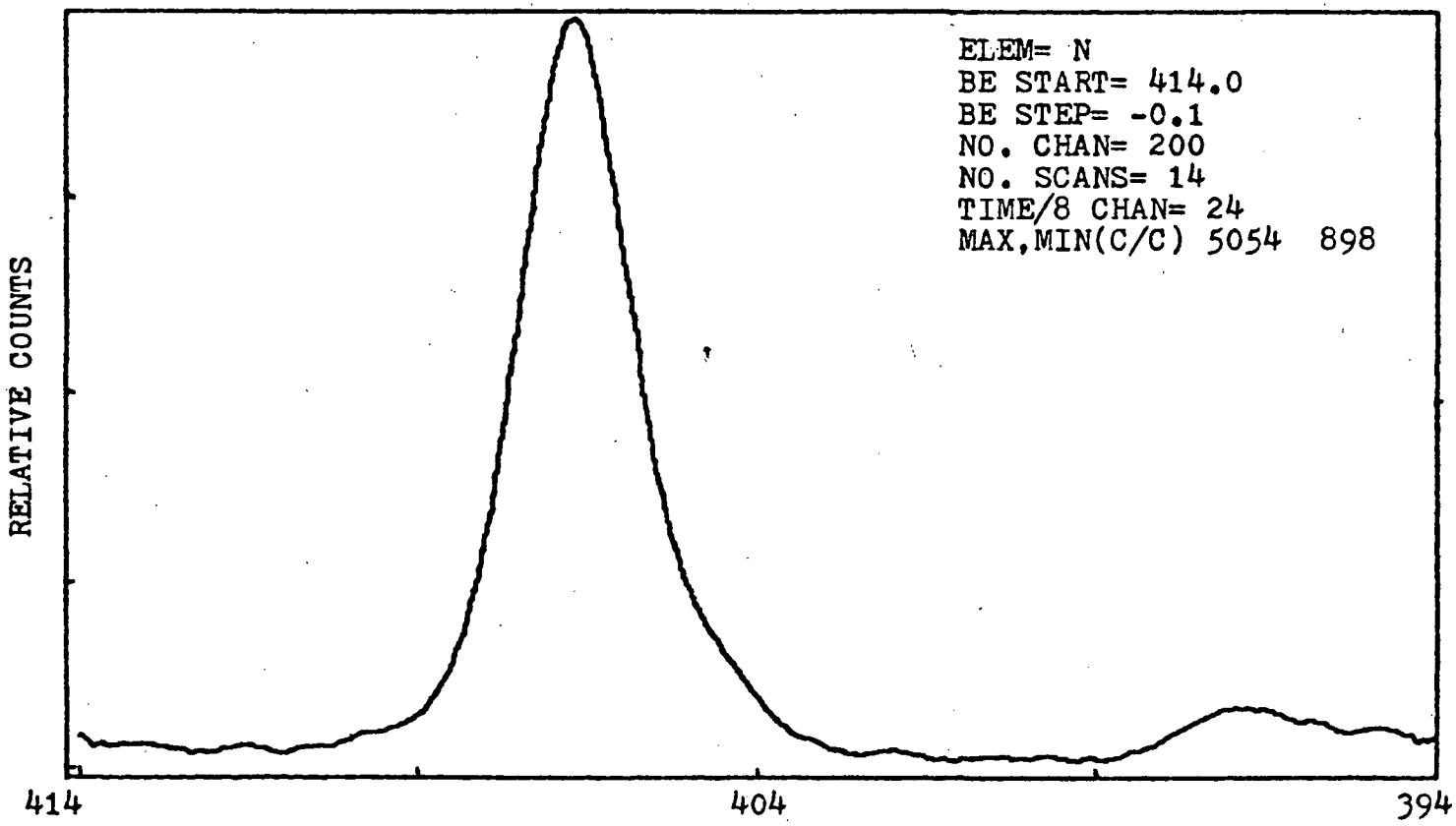

FIGURE 14 ESCA SPECTRUM OF N IN $(NH_4)_2SO_4$ COATED PYREX

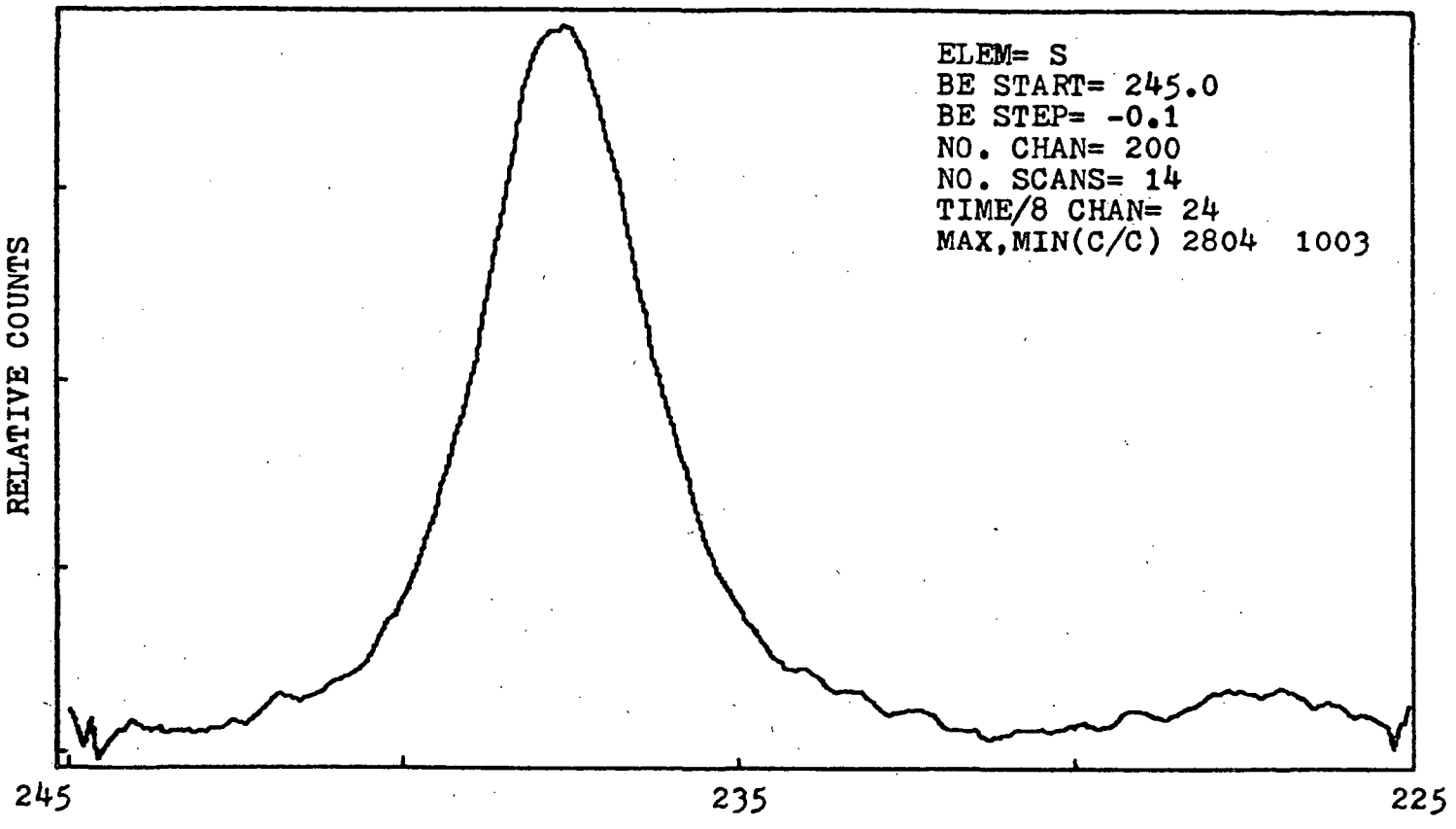

FIGURE 15 ESCA SPECTRUM OF S IN $(NH_4)_2SO_4$ COATED PYREX

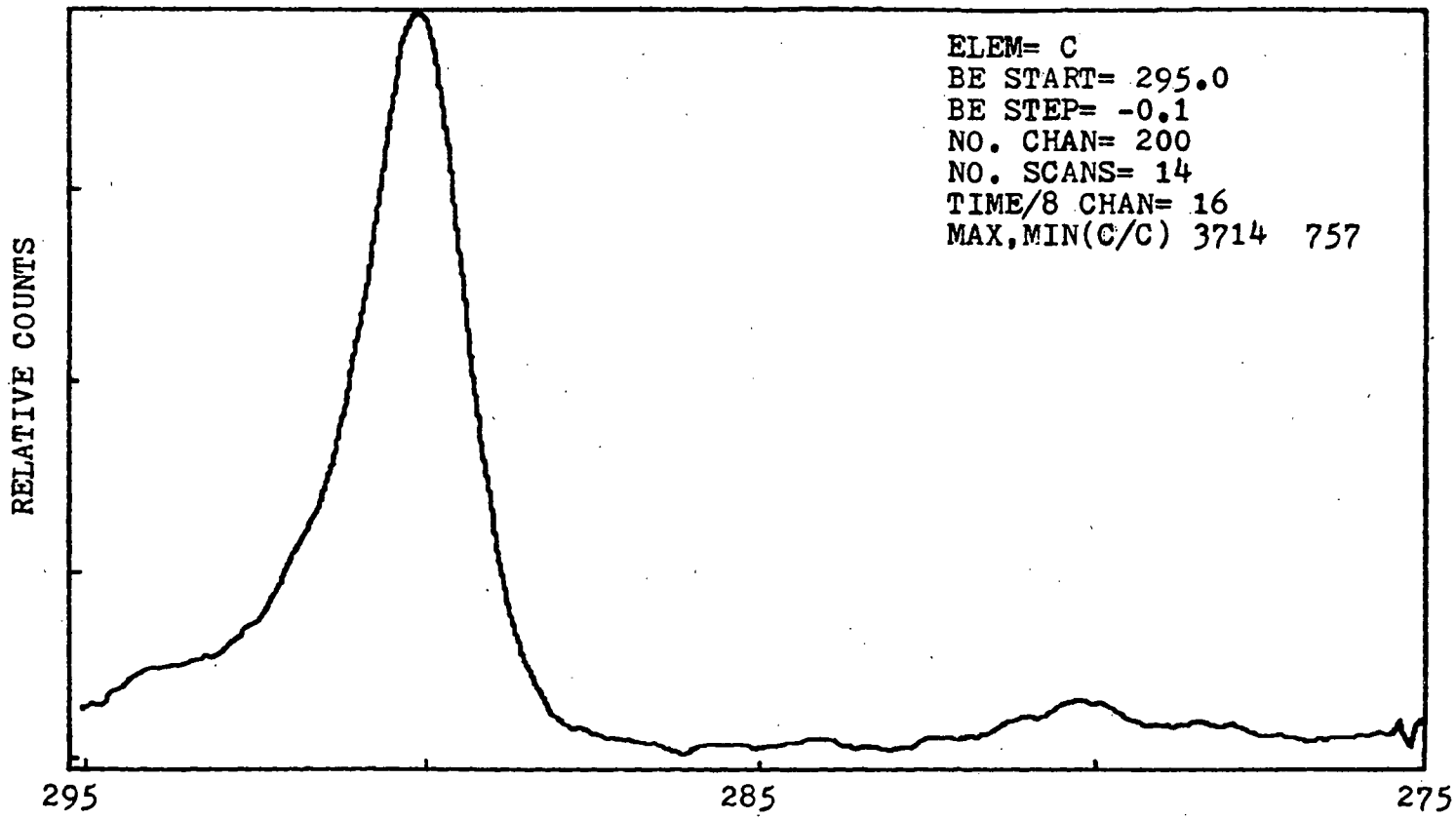

FIGURE 16 ESCA SPECTRA OF C IN $(NH_4)_2SO_4$ COATED PYREX

TABLE XIII

BINDING ENERGIES (eV) OF ELEMENTS IN PYREX

Sample	BINDING ENERGY (eV) FOR ELEMENT:				
Treatment	Si	O	S	N	C
None	103.4	532.6	MP[a]	400.0	285.0
HNO_3 wash	103.5	532.7	MP	MP	285.0
$(NH_4)_2SO_4$ coat	103.9	531.8	232.6	401.7	285.0
Full treatment	103.5	532.8	MP	MP	285.0

[a]Denotes a marginal peak

TABLE XIV

RELATIVE ESCA PEAK INTENSITIES

(Δ/min. scan)

Treatment	Element				
	Si	O	S	N	C
None	.479	.713	.0120	.0411	.446
HNO_3 wash	.740	1.36	.0120	.0200	.505
$(NH_4)_2SO_4$ coat	.125	.903	.128	.330	.279
Full Treatment	.724	1.69	.0194	.0348	.411

$(NH_4)_2SO_4$ film apparently partially covers the Pyrex surface. A strong N peak was found for the $(NH_4)_2SO_4$ coated glass. HNO_3 wash certainly decreased the intensity of the N signal of the untreated Pyrex.

Variations in k_{WALL} for a clean reactor, as reflected in the k_{WALL} error band, can be seen in Table IX. There was no significant systematic change in surface composition from the ESCA spectra to account for these variations in k_{WALL}.

CHAPTER V

CONCLUSIONS

The following conclusions were based on a study of the kinetics and modes of disappearance of oxygen atoms, with and without aerosols present:

1. The value of k_{WALL} for atomic oxygen on a clean Pyrex reactor was determined to be $2.3 \pm .7$ sec^{-1}.

2. The value of k_{WALL} for an H_2SO_4 coated Pyrex reactor was determined to be $.95 \pm .03$ sec^{-1}.

3. The value of k_{WALL} for an $(NH_4)_2SO_4$ coated Pyrex reactor was determined to be $.88 \pm .18$ sec^{-1}.

4. No detectable chemical reaction took place between $(NH_4)_2SO_4$ and atomic oxygen under the experimental conditions.

5. Measurement of k_{WALL} for an NH_4Cl coated Pyrex reactor was precluded by a fast exothermic reaction occuring between $NH_4Cl(s)$ and atomic oxygen.

6. The products of the reaction between $NH_4Cl(s)$ and atomic oxygen were determined to be NH_3, H_2O, NO, and HCl.

7. The value of k_{GAS}, for homogeneous atomic oxygen recombination, was determined to be $(1.46 \pm .61) \times 10^8$ $l^2/mol^2 sec$.

8. An NH_4Cl aerosol was produced by gas phase reaction of NH_3 plus HCl. The particles were approximately

spherical and nearly monodisperse with a diameter of $1.6 \pm .2\ \mu m$.

9. The value of k_{AERO} for atomic oxygen and NH_4Cl aerosol was determined to be $2.7 \pm .5\ sec^{-1}$.

10. An $(NH_4)_2SO_4$ aerosol was produced by vapor phase reaction of H_2SO_4 plus NH_3. The particles were irregularly shaped and the smallest particles had a diameter of about $2\ \mu m$.

11. The value of k_{AERO} for atomic oxygen and $(NH_4)_2SO_4$ aerosol was determined to be $< 0.5\ sec^{-1}$.

12. The model for aerosol-gas interaction kinetics proposed by Judeikis and Siegel to estimate k_{AERO} seems to merit further study.

13. There were variations in k_{APP} values for clean Pyrex wall after successive treatments and cleanings. No changes in surface composition of treated Pyrex could be detected by ESCA to account for the observed variations.

LITERATURE CITED

(1) L. V. Berkner and L. C. Marshall, J. Atmos. Sci. 22, 225 (1965).

(2) P. Crutzen, Can. J. Chem. 52, 1569 (1974).

(3) M. I. Ratner and J. C. G. Walker, J. Atmos. Sci. 29, 803 (1972).

(4) C. E. Junge, C. W. Chagnon, and J. E. Manson, J. Meteorol. 18, 81 (1961).

(5) S. C. Mossop, Nature 199, 325 (1963).

(6) S. I. Rasool and S. H. Schneider, Science 173, 138 (1971).

(7) M. Nicolet, Can. J. Chem. 52, 1381 (1974).

(8) S. Chapman, Quart. J. Roy. Meteorol. Soc. 3, 103 (1930), cited by H. J. Sanders, Chem. Eng. News 44, 1 (1966).

(9) H. U. Dutsch, "Chemical Reactions in the Lower and Upper Atmosphere", John Wiley and Sons, New York, 1961, p 167.

(10) H. K. Paetzold, ibid., p 181.

(11) L. J. Carter, Science 169, 660 (1970).

(12) H. Harrison, Science 170, 734 (1970).

(13) H. S. Johnston, Science 173, 517 (1971).

(14) H. I. Schiff, Ann. Geophys. 25, 815 (1969).

(15) C. E. Junge, Quart. J. Roy. Meteorol. Soc. 98, 711, (1972).

(16) P. J. Crutzen, J. Geophys. Res. 76, 7311 (1971).

(17) K. H. Welge, Can. J. Chem. 52, 1424 (1974).

(18) F. Kaufman, Prog. Reaction Kinetics 1, 1 (1961).

(19) R. J. Donovan, D. Husain, and L. J. Kirsch, Trans. Faraday Soc. 66, 2551 (1970).

(20) M. J. Ball and F. S. Larkin, Nature Phys. Sci. 245, 63 (1973).

(21) H. S. Johnston, "Gas Phase Reaction Kinetics of Oxygen Species", National Bureau of Standards NSRDS-20, U. S. Government Printing Office, Washington, D. C., 1968.

(22) R. E. Huie, J. T. Herron and D. D. Davis, J. Phys. Chem. 76, 2653 (1972).

(23) C. W. von Rosenberg and D. W. Trainor, J. Chem. Phys., 59, 2142 (1973).

(24) J. P. Wightman, Proc. IEEE 62, 4 (1974).

(25) B. A. Thrush, Science 156, 470 (1967).

(26) F. Kaufman, "Chemical Reactions in Electrical Discharges", Advances in Chemistry Series, No. 80, American Chemical Society, Washington, D. C., 1969, p 42.

(27) A. T. Bell and K. Kwong, Ind. Eng. Chem., Fundam. 12, 90 (1973).

(28) S. Krongelb and M. W. P. Strandberg, J. Chem. Phys., 31, 1196 (1959).

(29) J. T. Herron and R. E. Huie, J. Phys. Chem. 73, 1326 (1969).

(30) K. Furukawa, E. W. Gray and E. A. Ogryzlo, Ann. N. Y. Acad. Sci. 171, 175 (1970).

(31) F. Kaufman, J. Chem. Phys. 28, 352 (1958).

(32) F. Kaufman, Proc. Roy. Soc., Ser. A 247, 123 (1958).

(33) M. L. Spealman and W. H. Rodebush, J. Amer. Chem. Soc. 57, 1474 (1935).

(34) A. M. Mearns and A. J. Morris, J. Phys. Chem. 74, 3999 (1970).

(35) I. R. Slagle, J. A. Samlaska, F. J. Pruss, Jr., and D. Gutman, J. Phys. Chem. 78, 208 (1974).

(36) M. F. R. Mulcahy, J. R. Steven, and J. C. Ward, J. Phys. Chem. 71, 2124 (1967).

(37) P. D. Francis, Brit. J. Appl. Phys. 2, 1717 (1969).

(38) M-N. Raphalen and M. H. Tchen, C. R. Acad. Sci., Paris, Ser. B. 271, 21 (1970).

(39) A. Gelb and S. K. Kim, J. Chem. Phys. 55, 4935 (1971).

(40) H. I. Schiff, Can. J. Chem. 47, 1903 (1968).

(41) F. Kaufman and J. R. Kelso, Disc. Faraday Soc. 37, 26 (1964).

(42) M. F. R. Mulcahy and D. J. Williams, Trans. Faraday Soc. 64, 59 (1968).

(43) M. A. A. Clyne, D. J. McKenney and B. A. Thrush, Trans. Faraday Soc. 61, 2701 (1965).

(44) A. Mathias and H. I. Schiff, J. Chem. Phys. 40, 3118 (1964).

(45) H. I. Schiff, Ann. Geophys. 20, 115 (1964).

(46) A. M. Mearns and A. J. Morris, Chem. Eng. Progr. Symp. Ser. 67, 37 (1971).

(47) M. A. A. Clyne, Phys. Chem. Fast React. 1, 245 (1973).

(48) D. J. Williams and M. F. R. Mulcahy, Aust. J. Chem. 19, 2163 (1966).

(49) C. E. Junge and J. E. Manson, J. Geophys. Res. 66, 2163 (1961).

(50) P. K. Mueller and E. L. Kothny, Anal. Chem. 45, 1 (1973).

(51) J. P. Friend, R. Leifer, and M. Trichon, J. Atmos. Sci. 30, 465 (1973).

(52) J. Bricard and D. Vigla, Can. J. Chem. 52, 1479 (1974).

(53) C. S. Kiang, D. Stauffer and V. A. Mohnen, Nature Phys. Sci. 244, 53 (1973).

(54) S. C. Wofsy and M. B. McElroy, Can. J. Chem. 52, 1582 (1974).

(55) R. S. Stolarski and R. J. Cicerone, Can. J. Chem. 52, 1610 (1974).

(56) M. W. First, Arch. Int. Med. 131, 24 (1973).

(57) R. E. Lee, Jr., Science 178, 567 (1972).

(58) N. A. Fuchs and A. G. Sutugin, "Topics in Current Aerosol Research," Part 2, G. M. Hidy and J. R. Brock, Eds., Pergamon Press Inc., New York, 1971, Chapter 1.

(59) A. Goetz and R. Pueschel, Atmos. Environ. 1, 287 (1967).

(60) R. N. Berglund and B. Y. H. Liu, Environ. Sci. Technol. 7, 147 (1973).

(61) B. Dahneke, Nature Phys. Sci. 244, 55 (1973).

(62) S. Twomey, J. Chem. Phys. 31, 1684 (1959).

(63) D. Scargill, Nature 247, 101 (1974).

(64) R. J. Countess and J. Heicklen, J. Phys. Chem. 77, 444 (1973).

(65) R. C. Robbins and R. D. Cadle, J. Phys. Chem. 62, 469 (1959).

(66) G. M. Hidy, "Surface and Colloid Science", Vol. 2, E. Matijevic, Ed., Wiley-Interscience, New York, 1969.

(67) W. E. Ranz and J. B. Wong, Ind. Eng. Chem. 44, 1371 (1952).

(68) M. N. Golovin and A. A. Putnam, Ind. Eng. Chem., Fundam. 1, 264 (1962).

(69) B. Dahneke, J. Colloid Interface Sci. 37, 342 (1971).

(70) B. Dahneke and H. Flachsbart, J. Aerosol Sci. 3, 345 (1972).

(71) S. K. Friedlander, Ind. Eng. Chem. 50, 1161 (1958).

(72) J. J. Olivero, J. Geophys. Res. 79, 476 (1974).

(73) A. P. Altshuller and J. J. Bufalini, Photochem., Photobiol. 4, 97 (1965).

(74) M. D. Carabine, Chem. Soc. Reviews 1, 411 (1972).

(75) J. Wagman, Air Water Pollut. 10, 777 (1966).

(76) M. Hirono, M. Fujiwara, O. Uchino, and T. Itabe, Can. J. Chem. 52, 1560 (1974).

(77) H. S. Judeikis and S. Siegel, Atmos. Environ. 7, 619 (1972).

(78) L. W. Barr, F. P. Koffyberg, and J. A. Morrison, J. Appl. Phys. 33, 222 (1962).

(79) H. F. Johnstone and D. R. Coughanour, Ind. Eng. Chem. 50, 1169 (1958).

(80) R. C. Robbins, R. D. Cadle and D. L. Eckhardt, J. Meteorol. 16, 53 (1958).

(81) R. D. Cadle, J. Colloid Interface Sci. 39, 25 (1972).

(82) W. C. Gardiner, Jr., "Rates and Mechanisms of Chemical Reactions," W. A. Benjamin, Menlo Park, California, 1972, p 26.

(83) Robert C. Weast (ed.), "Handbook of Chemistry and Physics," 48th ed, Chemical Rubber Co., Cleveland, Ohio, 1968, p D-117.

(84) J. C. Greaves and J. W. Linnett, Trans. Faraday Soc. 55, 1346 (1959).

(85) D. Garvin, ed., "Chemical Kinetics Data Survey IV. Preliminary Tables of Chemical Data for Modelling of the Stratosphere," National Bureau of Standards IR-203, U. S. Governmental Printing Office, Washington, D. C., 1973.

(86) D. M. Hercules and J. C. Carver, Anal. Chem. 46, 133R (1974).

(87) W. P. Dianis and J. E. Lester, Anal. Chem. 45, 1416 (1973).

APPENDIXES

APPENDIX I

ERROR ANALYSIS AND DISCUSSION

Error Associated With The Flow System

Each of the three assumptions discussed in Chapter II will be examined to see if they are reasonable in this study.

Assumption of negligible pressure drop over the titration region: From equation [27], it can be seen that as the flow velocity increases, so does the pressure drop. On this basis, it would seem better to use slow flows. Slow flows, however, allow back diffusion into the discharge. When this occurs, great uncertainties arise as to what species form and what reactions they undergo. High flow velocities, controlled by the pumping speed and the desired system pressure, were used. For the wall recombination studies, the titration region was about 30 cm long. Substituting the value for the highest flow velocity used, 674 cm/sec. into equation [27], we find $\Delta P = 0.05$ torr. The system pressure corresponding to this flow was 1.3 torr, giving an overall pressure drop of 3.8%. For the aerosol system, a longer titration region was used. For this 60 cm titration region, operated at a flow

velocity of 769 cm/sec at 1.5 torr, the calculated pressure drop was 0.12 torr, an overall change of 8%. These pressure uncertainties were considered a small price to pay to eliminate back diffusion.

Assumption of negligible back diffusion: This has been discussed somewhat in part 1 above. The relation to be satisfied is given in Chapter II as equation [28]. Assuming $D = 270\ cm^2/sec$, $k = 1\ sec^{-1}$, and $u = 303\ cm\ sec^{-1}$, the slowest flow used, the inequality reads $0.0029 << 1$. This agrees with the visual observation of no back diffusion into the discharge.

Assumption of small radial concentration gradients: This assumption was believed valid because of the similarity of the system used to the one analysed by Kaufman (18). Radial concentration gradients arise if wall recombination is very fast, but are less than 1% in a 2 cm diameter flow tube if k_{WALL} is less than $5\ sec^{-1}$. The system used in this study had a diameter less than 2 cm and k_{WALL} never exceeded $5\ sec^{-1}$. On this basis, radial concentration gradients were assumed negligible.

Error in Elapsed Time Values and Sample Calculation

The example chosen is that having the greatest uncertainty. The volume of bulb B1 was found by measuring the

pressure drop as gas expanded from a known volume. Pressure was measured by mercury manometer read to ±.5 mm. The bulb volume and error, computed in the usual way, was 5317 cm^3 (±2%). To maintain a system pressure of 1.50 torr, the bulb pressure dropped 100 mm (±.4%) in a time period of 318 sec (±1.6%). The time error was assumed on the basis of a ±5 sec uncertainty as to when to stop the timer. This gave a value of $\Delta P/\Delta t$ = .314 torr/sec (±2%). The volume flow rate was then found, where

$$\Delta V/\Delta t = (\Delta P/\Delta t)(V)/P$$
$$= (.314 \pm 2\%)(5317 \pm 2\%)/1.50 \pm 1\%$$
$$= 1113 \text{ cm}^3/\text{sec } (\pm 5\%).$$

Converting to linear flow velocity,

$$\Delta x/\Delta t = (\Delta V/\Delta t)/A,$$

where A is the flow tube cross-sectional area. From a measured tube i.d. = 1.36 ± .01 cm, the area A = 768 cm/sec (±5.74%). Then, for the smallest distance increment, Δx = 10.15 cm (±.2%), giving an elapsed time of 1.32×10^{-2} sec (±6%).

Error in NO_2 Titrant Gas Flows

The NO_2 flow, in moles per second, was determined in a manner similar to the O_2 flow. Flow was measured by a capillary flowmeter, however, and required long times to allow a significant pressure drop. For tube H194, the point

at FMR = 18.9 is considered as an example. The value of ΔP was 10.0 ± .1 mm (±2%), for a Δt = 5746 ± 60 sec (±1%). Substituting,

$$\Delta n/\Delta t = (\Delta P/\Delta t)(V)/RT$$
$$= (1.74 \times 10^{-3} \pm 3\%)(5369 \pm 2\%)/(62400)(300 \pm .3\%)$$
$$= 5.0 \times 10^{-7} \text{ moles/sec } (\pm 5.3\%).$$

As the NO_2 working curve was constructed, an error bar of 5% was put on each point. There was no difficulty in fitting a smooth curve to all the data points.

By using flow ratios as a basis for calculating k_{APP}, uncertainties due to the NO_2--N_2O_4 equilibrium were assumed to cancel out.

Error in Rate Constant Values

For kinetic determinations as in this study, it is very difficult to calculate an error for the rate constant from individual errors. This is due mainly to the inability to evaluate some of those individual errors. Two examples are (a) NO_2 flowmeter reading, especially since it oscillates over a 0.1--0.2 unit range at times; and (b) estimation of the point of maximum intensity from the photodetector reading. Thus, uncertainties quoted for k_{APP} values come from statistical analysis of the ln R versus t plots. By simultaneous computer least squares analysis of several sets of points a one-standard-deviation

error in the slope is found which reflects the uncertainties in the measurement. Errors quoted for k_{WALL}, k_{GAS}, and k_{AERO} are also one standard deviation, either computer calculated or found from the relation

$$\sigma = [(\Sigma d^2/N) - (\Sigma d/N)^2]^{\frac{1}{2}}$$

where, for a set of values, d is the deviation from the mean value and N is the number of values.

APPENDIX II

"FOCAL" PROGRAM USED FOR RATE CONSTANT CALCULATIONS[a]

```
1.05 T !!!!!!!! "  FRANK'S FAST FIRST-ORDER FORMULATOR,!
1.07 T " (BASED ON LINEAR LEAST SQUARES)",!!
1.10 A "DATE, B, "  COMMENTS", Z, !!
1.15 A "NUMBER OF POINTS", N, !!
1.16 S P= 0; S Q=0; S R= 0; S S=0; S W=0
1.17 A "K-APPARENT OR K-GAS", K, !!!
1.19 I (1-K)2.05, 3.05

2.05 T "   P 2(TORR↑2)          K-APP(SEC↑-1)",!
2.10 F I=1,n; DO 5.00
2.15 D 6.00
2.20 T %, ! "K-GAS",(SL/2), " TORR↑-2SEC↑-1  ERROR",DM/2,!
2.25 T %, "  ",(SL*3.46*10↑8)/2, " LITER↑2MOLE↑-2SEC↑-1"
2.30 T %,!! " K-WALL", IN," PER SEC.  ERROR", DB,!!!
2.35 A " ANOTHER", A, !!!!!!!!
2.40 I (A-25)7.6,1.15

3.05 T "  TIME(SEC)  (0) T/(0) 0"; A "    PRESSURE(TORR)", M,!
3.10 F I=1,N; DO 4.00
3.15 D 6.00
3.20 T %4.03, "K-APPARENT", (-1*SL), " SEC↑-1  ERROR",DB,!
3.25 T %, "ERROR IN LN R", DY,!!
3.30 A " ANOTHER", A, !!!!!!!!
3.35 I (A-25)7.6, 1.15

4.05 A "     ",T,"     ",C,!
4.07 S X(I)=T; S Y(I)=FLOG(C)
4.10 S P=P+X(I); S Q=Q+Y(I)
4.15 S R=R+X(I)*X(I); S S=S+X(I)*Y(I); S W=W+Y(I)*Y(I)

5.05 A "    ",X(I),"    ",Y(I),!
5.15 S P=P+X(I); S Q=Q+Y(I)
5.20 S R=R+X(I)*X(I); S S=S+X(I)*Y(I); S W=W+Y(I)*Y(I)

6.05 S NS=(N*S-P*Q)
6.10 S D=N*R-P*P
6.15 S NI=R*Q-P*S
6.20 S SL=NS/D; S IN=NI/D
6.25 D 7.00

7.05 S RS=SL*(NS/N); S TS=W-(Q*Q)/N
7.10 S SS=TS-RS; S SQ=SS/(N-S)
7.15 S DM=FSQT(SQ/(D/N)); S DY=FSQT(SQ)
7.20 S DB=FSQT((SQ*R)/D)
7.25 R
7.60 Q
```

[a]Based on a program supplied by Dr. P. E. Field

APPENDIX III

KINETIC DATA: RECOMBINATION ON CLEAN WALL

Runs Performed 9-4-73 through 9-6-73[a]

Run Number	Pressure (torr)	FMR J1	J2	J3	J4
0.50C	0.50	23.0	22.0	21.0	20.0
0.50D		23.0	21.5	20.5	20.0
0.50E		23.0	21.5	20.5	20.0
0.50G		24.5	23.0	22.0	21.0
0.50M		27.0	26.0	25.0	24.0
0.80A	0.80	37.0	35.0	34.0	32.0
0.80B		37.0	36.0	34.0	32.0
0.80C		37.0	35.0	34.0	32.0
0.80D		39.0	37.0	35.0	34.5
1.0A	1.00	43.0	42.0	41.0	40.0
1.0B		43.0	42.0	40.0	39.0
1.0C		39.0	38.0	37.0	36.0
1.0D		49.0	48.0	46.0	45.0
1.0E		40.0	37.0	35.0	34.0
1.0F		40.0	39.0	37.0	36.0
1.0G		37.0	36.0	34.0	36.0
1.3A	1.30	51.0	50.0	48.0	46.0
1.3B		51.0	49.0	48.0	46.0
1.3C		57.0	55.0	54.0	52.5
1.3D		53.0	50.0	49.0	47.0

[a]See Table II for elapsed time data for these runs.

APPENDIX IV

KINETIC DATA: ATOM RECOMBINATION ON $(NH_4)_2SO_4$ COATED WALL

Runs Performed 9-10-73 through 9-11-73[a]

Run Number	Pressure (torr)	FMR J1	J2	J3	J4
C.50A	0.50	24.5	23.5	22.5	22.0
C.50B		24.5	23.5	22.5	22.0
C.50C		24.0	23.0	23.0	21.0
C.50D		21.5	20.5	19.5	19.0
C.50E		23.0	22.0	21.5	21.0
C.50F		24.0	23.0	22.0	21.5
C.80A	0.80	43.0	42.0	41.0	40.0
C.80B		45.0	44.5	43.5	42.5
C.80C		44.0	43.0	42.5	42.0
C.80D		44.0	43.0	42.5	41.5
C.80E		45.0	44.0	43.5	42.5
C.80F		44.0	43.0	43.0	42.0
C1.0A	1.00	51.0	50.0	49.0	49.0
C1.0B		51.0	50.0	49.0	49.0
C1.0C		51.0	50.0	49.5	49.0
C1.0D		52.0	51.0	50.0	49.5
C1.3A	1.30	60.0	58.0	58.0	57.0
C1.3B		65.6	65.0	64.0	63.0
C1.3C		63.0	61.5	61.0	60.0

[a]See Table II for elapsed time data for these runs

APPENDIX V

KINETIC DATA: RECOMBINATION ON H_2SO_4 COATED WALL

Runs Performed 9-14-73 through 9-17-73[a]

Run Number	Pressure (torr)	FMR J1	J2	J3	J4
S.50A	0.50	20.0	19.5	19.0	18.5
S.50B		20.0	19.5	19.0	18.5
S.50C		25.0	24.5	23.0	23.0
S.50D		26.5	26.0	25.0	24.5
S.50E		23.0	22.5	22.0	21.5
S.80A	0.80	38.0	37.5	37.0	36.0
S.80B		37.0	36.0	36.0	35.5
S.80C		38.0	38.0	37.0	36.0
S.80D		37.0	36.5	36.0	35.5
S1.0A	1.00	55.5	55.0	55.0	53.5
S1.0B		60.0	59.0	58.5	58.5
S1.0C		59.0	58.0	57.5	57.0
S1.0D		55.0	55.0	54.0	53.5
S1.0E		50.0	49.0	48.6	48.0
S1.0F		51.0	50.5	50.0	49.5
S1.3A	1.30	63.8	63.0	62.5	62.0
S1.3B		64.5	64.0	63.5	63.0
S1.3C		64.5	64.0	63.0	63.0

[a]See Table II for elapsed time data for these runs.

APPENDIX VI

KINETIC DATA: RECOMBINATION ON CLEAN WALL[a]

Date Performed: 6-4-74

Run Number	Pressure (torr)	FMR J1	J2	J3	J4
2	0.80	22.0	18.5	16.0	15.0
3		22.0	18.0	16.0	15.0
4		21.0	18.0	15.5	14.5
5	1.00	26.5	23.5	22.0	20.5
6		26.5	23.5	22.0	20.0
7		26.5	23.5	22.0	20.5
8	1.30	32.0	30.0	27.5	25.5
9		33.0	29.5	27.5	26.0
10		33.0	29.5	27.5	26.0
11	1.50	35.0	32.5	30.0	28.5
12		36.5	33.0	30.5	28.5
13		35.0	31.5	29.5	28.0
	Date Performed: 6-6-74				
1	1.50	35.0	32.0	30.0	27.0
2		34.5	31.5	29.0	27.0
3	1.00	23.0	19.5	17.0	15.5
4		23.5	19.5	17.0	15.5
5	1.30	28.5	26.0	25.0	21.5
6		29.5	26.0	23.0	21.5
7		28.5	26.0	23.0	21.0

[a]See Table IV for elapsed time data for these runs.

APPENDIX VI (continued)

KINETIC DATA: RECOMBINATION ON CLEAN WALL[a]

Date Performed: 6-12-74

Run Number	Pressure (torr)	J1	J2	J3	J4
1	1.50	31.0	29.0	28.0	25.5
2		32.0	29.5	27.5	26.0
3		32.0	29.5	28.0	25.5
4	1.30	27.0	24.5	22.0	20.0
5		27.0	25.0	23.0	22.0
6		28.0	25.5	24.0	22.5
7	1.00	18.0	16.5	15.5	14.5
8		19.5	17.5	16.0	15.0
	Date Performed: 6-14-74				
1	1.5	37.0	34.5	34.0	33.0
2		37.0	36.0	35.0	33.0
3		37.5	35.5	34.5	34.0
4	1.00	26.5	25.0	23.5	23.0
5		27.0	25.0	24.0	23.0
6		27.5	25.5	25.0	23.5
8	1.30	35.0	33.0	31.5	30.5
9		34.0	32.0	31.0	30.0
10	0.80	19.5	18.0	17.0	16.5
11		20.0	18.5	17.5	16.5

[a]See Table IV for elapsed time data for these runs.

APPENDIX VII

KINETIC DATA: NH_4Cl AEROSOL RUNS[a]

Run Number	Condition	FMR J1	J2	J3	J4
6-24-6	Pre-sol	19.0	18.5	18.0	17.5
-7A	NH_4Cl	19.0	18.2	18.0	17.5
-8	Post-sol	18.5	18.0	17.5	17.0
7- 2-6	Pre-sol	25.0	23.5	22.0	20.0
-7A	NH_4Cl	24.5	23.5	22.8	21.5
-8	Post-sol	24.5	24.0	23.5	23.0
7- 2-10	Pre-sol	24.5	23.5	23.0	22.5
-11A	NH_4Cl	23.0	21.5	20.0	19.5
-12	Post-sol	23.0	22.5	22.5	22.0
7- 3-9	Pre-sol	24.5	24.0	23.5	22.0
-10A	NH_4Cl	22.0	20.0	18.5	17.0
-11	Post-sol	23.0	23.0	23.0	22.5
7- 6-6	Pre-sol	18.5	18.5	18.0	17.5
-7A	NH_4Cl	18.5	18.0	17.5	17.0
-8	Post-sol	18.5	18.0	18.0	18.0
7- 6-9A	NH_4Cl	18.5	17.5	17.0	15.5
-10	Post-sol	18.5	18.0	18.0	18.0

[a]See Table IV for elapsed time data for these runs.

APPENDIX VII (continued)[a]

Run Number	Condition	FMR J1	J2	J3	J4
7-6-11A	NH_4Cl	18.5	18.0	17.5	17.0
-12	Post-sol	18.5	18.0	18.0	18.0
7-6-17A	NH_4Cl	20.0	18.0	17.0	15.0
-18	Post-sol	20.0	20.0	20.0	20.0

[a]See Table IV for elapsed time data for these runs.

APPENDIX VIII

KINETIC DATA: EFFECT OF EXCESS FLOWS OF NH_3 OR HCl[a]

Run Number	Added Gas : FMR	FMR J1	J2	J3	J4
6-18-5		20.2	19.8	19.2	18.5
6-18-6		20.2	19.5	19.0	18.5
6-18-7N	NH_3 : 1.0	22.0	20.5	20.0	19.8
6-18-8N	NH_3 : 1.0	22.5	21.0	20.2	20.0
6-18-9		20.5	20.0	19.0	18.2
6-18-10		20.0	19.5	19.0	19.0
6-19-10		25.0	22.5	20.5	19.0
6-1911N	NH_3 : 1.0	25.0	22.5	22.0	20.5
6-19-12		25.0	23.0	21.5	20.5
6-20-2		18.5	17.2	16.0	15.0
6-20-3		18.0	17.0	16.0	15.0
6-20-4N	NH_3 : 1.0	18.3	18.0	17.0	15.5
6-20-5N	NH_3 : 1.0	18.5	18.2	17.0	16.0
6-20-6N	NH_3 : 1.0	18.5	18.0	17.5	16.5
6-20-7N	NH_3 : 1.0	19.0	18.0	17.5	16.5
6-20-8		19.5	19.0	18.0	16.5

[a]See Table IV for elapsed time data for these runs.

APPENDIX VIII (continued)

Run Number	Added Gas : FMR	FMR J1	J2	J3	J4
6-21-5		18.0	17.5	17.0	16.5
6-21-6		18.0	17.5	17.2	16.5
6-21-7H	HCl : 1.0	18.0	17.0	16.8	16.2
6-21-8H	HCl : 1.0	18.0	17.2	17.0	16.5
6-21-9		18.0	17.5	17.0	16.5
6-21-10H	HCl : 1.0	18.0	17.5	17.0	16.5
6-21-11		18.5	18.0	17.5	17.0

APPENDIX IX

KINETIC DETERMINATIONS WITH $(NH_4)_2SO_4$ AEROSOL PRESENT

Aerosol Generation and Characterization

The $(NH_4)_2SO_4$ aerosol was generated as described in Chapter III - EXPERIMENTAL (pp 36-41). The H_2SO_4 boiler was operated between 200-205 ^oC corresponding to a mean vapor pressure of 14.5 torr. The flow rate of NH_3 was about one-half the value used in the generation of the NH_4Cl aerosol. Copious quantities of white aerosol were observed to form in the generator bulb on mixing NH_3 with H_2SO_4 vapor. The particle concentration of the $(NH_4)_2SO_4$ aerosol was estimated, as in the case of NH_4Cl, by measuring the mass of the aerosol collected after varying collection times. Particle concentration values from several runs are given in Table XV. The temperature of the H_2SO_4 boiler and the FMR values for the NH_3 source are both indicated in the third column. A cursory comparison of the results in Table XV with the results for the NH_4Cl aerosol in Table VI indicates that much greater amounts of the $(NH_4)_2SO_4$ aerosol were collected. A straight line was obtained when the mass of $(NH_4)_2SO_4$ collected was plotted versus collection time as shown in Figure 17. The slope of the line was 233 $\mu g/sec$. A particle concentration of 285 x 10^3 $\mu g/m^3$ was calculated from the ratio of mass collected per unit time to volume

TABLE XV

$(NH_4)_2SO_4$ AEROSOL PRODUCTION DATA

Date	Run #	Temp/FMR	Aerosol Exposure (sec)	Aerosol Mass Collected (g)
10/19/74	1	205/7.5	154	0.0097
	2	206/7.0	246	0.0411
	3	203/7.0	150	0.0176

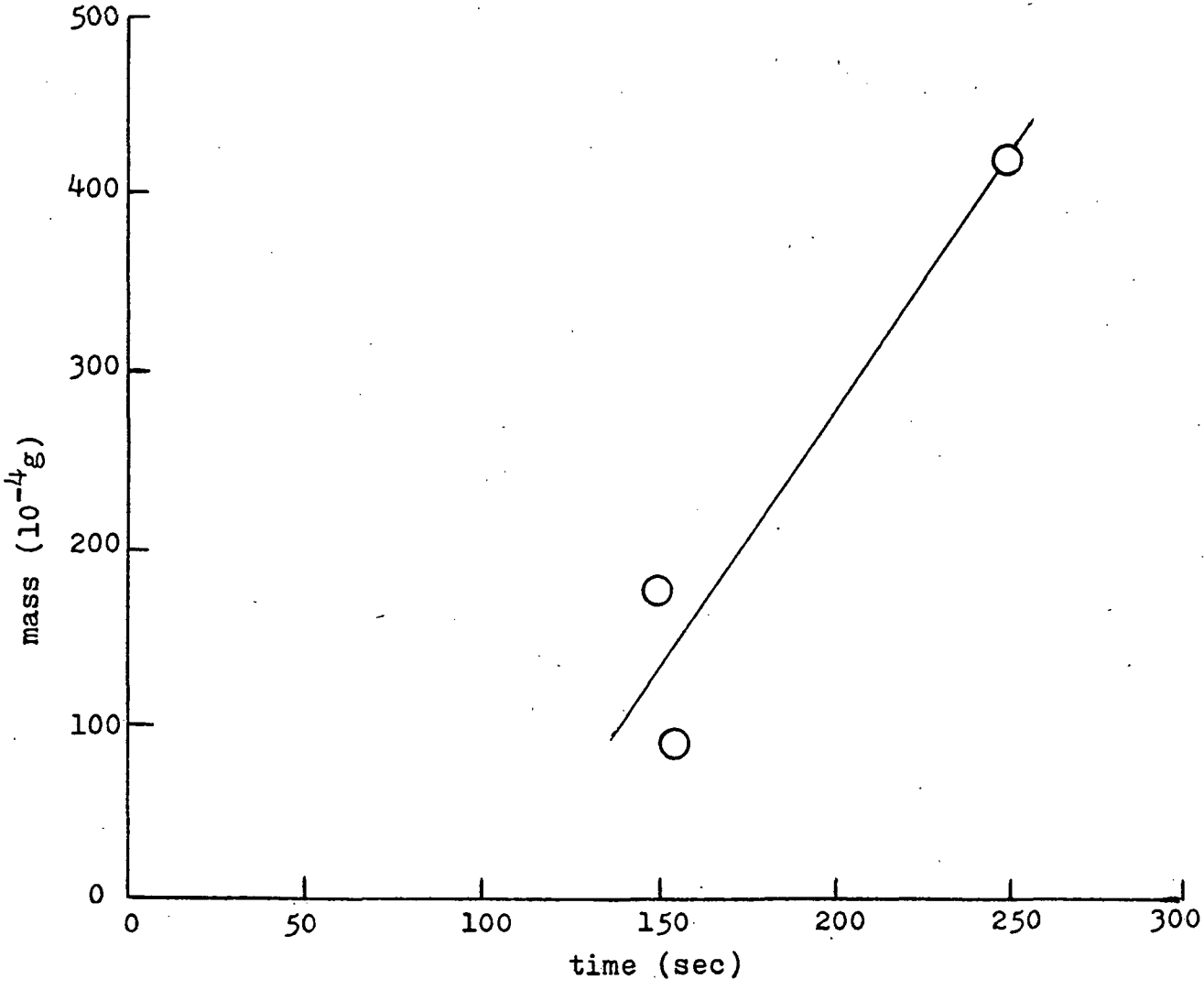

FIGURE 17 PLOT OF $(NH_4)_2SO_4$ AEROSOL MASS COLLECTED VERSUS TIME

flow rate. A scanning electron photomicrograph of the collected particles taken at 4800X is shown in Figure 18. The $(NH_4)_2SO_4$ particles are irregularly shaped and the diameter of the smallest particles just to the left of center have an average diameter of 2 μm. X-ray analysis (EDAX) of the particles in the beam of the scanning electron microscope confirmed the presence of sulfur in the particles. The irregularly shaped $(NH_4)_2SO_4$ particles are in morbid contrast to the nearly spherical NH_4Cl particles (Figure 9).

Kinetic Determinations with Aerosol Present - $(NH_4)_2SO_4$

The $(NH_4)_2SO_4$ aerosol was run at a system pressure of 1.5 torr. Atom concentrations were measured in the same way as described above. Data for the $(NH_4)_2SO_4$ aerosol runs are given in Table XVI. The temperature of the H_2SO_4 boiler and the FMR value of the NH_3 source are indicated after each aerosol run. The very significant result was that there was no detectable decrease in the concentration of atomic oxygen in the presence of the $(NH_4)_2SO_4$ aerosol. Thus, k_{AERO} was taken to be < 0.5 sec^{-1}. A value of 0.5 sec^{-1} for k_{AERO} corresponds to a just measureable decrease in atomic oxygen with the present apparatus using NO_2 titration. This result is in marked contrast to the results for the NH_4Cl aerosol where a pronounced effect of the aerosol on the rate constant was observed. The model of Judeikis and Siegel (77) was used to again check agreement with the experimental

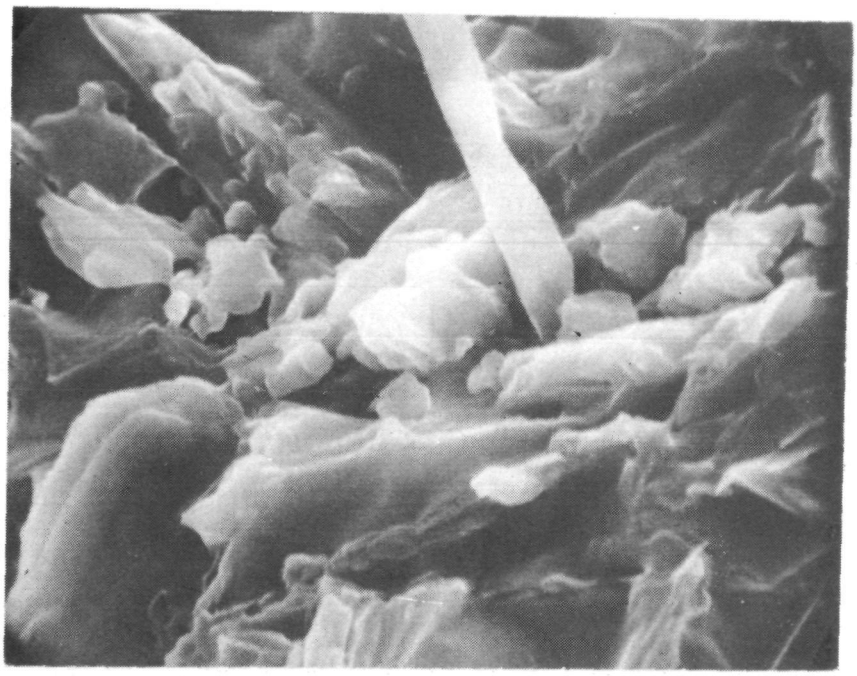

FIGURE 18

PHOTOMICROGRAPH OF $(NH_4)_2SO_4$ AEROSOL PARTICLES

TABLE XVI

KINETIC DATA: $(NH_4)_2SO_4$ AEROSOL RUNS

Run Number	Condition	FMR J1	J2	J3	J4
8-24-4	Pre-sol	41.0	41.0	40.5	40.5
8-24-5A	Aerosol: 200/7.5	40.0	40.0	40.0	39.5
8-24-1	Pre-sol	44.0	44.0	44.0	44.0
8-24-2A	Aerosol: 205/7.0	43.0	43.0	43.0	43.0
8-24-3	Post-sol(Δt=1min)	43.0	43.0	43.0	43.0
8-15-1	Pre-sol	31.5	31.5	31.5	31.5
8-15-2A	Aerosol: 200/2.5	31.0	31.0	30.0	30.0
8-15-3	Post-sol(Δt=1 min)	31.0	31.0	31.0	30.5

observation of a negligible value of k_{AERO}. A value of k_{CALC} was calculated using equation [35], setting $W = 285 \times 10^{-6}$ kg/m^3, $\rho = 1769$ kg/m^3, $r_m = 1 \times 10^{-4}$ cm, $M_G = 16$ g/mol, $\gamma = 2$, $\Phi = 1.9 \times 10^{-5}$ and $T = 300$ °K. The value of Φ was taken from the measured wall recombination rate on a $(NH_4)_2SO_4$ coating (see Table IX). The calculated value of k_{CALC} was 3×10^{-3} sec^{-1} which represents a rate constant too small to produce a detectable decrease in the atomic oxygen concentration as determined by the NO_2 titration technique. Again, as was true in the case of NH_4Cl aerosol, the model of Judeikis and Siegel is in qualitative agreement with the experimental results and the model certainly merits further experimental verification.

NATIONAL AERONAUTICS AND SPACE ADMINISTRATION
WASHINGTON, D.C. 20546

OFFICIAL BUSINESS
PENALTY FOR PRIVATE USE $300

SPECIAL FOURTH-CLASS RATE
BOOK

POSTAGE AND FEES PAID
NATIONAL AERONAUTICS AND
SPACE ADMINISTRATION
451

U.S.MAIL

POSTMASTER: If Undeliverable (Section 158 Postal Manual) Do Not Return

"The aeronautical and space activities of the United States shall be conducted so as to contribute . . . to the expansion of human knowledge of phenomena in the atmosphere and space. The Administration shall provide for the widest practicable and appropriate dissemination of information concerning its activities and the results thereof."

—NATIONAL AERONAUTICS AND SPACE ACT OF 1958

NASA SCIENTIFIC AND TECHNICAL PUBLICATIONS

TECHNICAL REPORTS: Scientific and technical information considered important, complete, and a lasting contribution to existing knowledge.

TECHNICAL NOTES: Information less broad in scope but nevertheless of importance as a contribution to existing knowledge.

TECHNICAL MEMORANDUMS: Information receiving limited distribution because of preliminary data, security classification, or other reasons. Also includes conference proceedings with either limited or unlimited distribution.

CONTRACTOR REPORTS: Scientific and technical information generated under a NASA contract or grant and considered an important contribution to existing knowledge.

TECHNICAL TRANSLATIONS: Information published in a foreign language considered to merit NASA distribution in English.

SPECIAL PUBLICATIONS: Information derived from or of value to NASA activities. Publications include final reports of major projects, monographs, data compilations, handbooks, sourcebooks, and special bibliographies.

TECHNOLOGY UTILIZATION PUBLICATIONS: Information on technology used by NASA that may be of particular interest in commercial and other non-aerospace applications. Publications include Tech Briefs, Technology Utilization Reports and Technology Surveys.

Details on the availability of these publications may be obtained from:

SCIENTIFIC AND TECHNICAL INFORMATION OFFICE

NATIONAL AERONAUTICS AND SPACE ADMINISTRATION

Washington, D.C. 20546